Supplemental Material

Enhanced Ca^{2+}-dependent SK-channel gating and membrane trafficking in human atrial fibrillation

Jordi Heijman, PhD*; Xiaobo Zhou, MD*; Stefano Morotti, PhD; Cristina E. Molina, PhD; Issam H. Abu-Taha, PhD; Marcel Tekook, PhD; Thomas Jespersen, PhD; Yiqiao Zhang; Shokoufeh Dobrev, PhD; Hendrik Milting, PhD; Jan Gummert, MD; Matthias Karck, MD; Markus Kamler, MD; Ali El-Armouche, MD; Arnela Saljic, PhD; Eleonora Grandi, PhD; Stanley Nattel, MD; Dobromir Dobrev, MD

*Shared first authorship

Corresponding Author:
Dobromir Dobrev, MD; Institute of Pharmacology, Hufelandstr 55, D-45122 Essen, Germany; Phone: +49-201-733-3477; Fax: +49-201-723-5593; E-mail: dobromir.dobrev@uk-essen.de

Contents

Comparison to previous literature

Table S1. AF-related remodeling of SK-channel mRNA and protein levels in the current study and as reported in the literature.

RA							
Reference	**Patients**	**mRNA KCNN1**	**KCNN2**	**KCNN3**	**Protein SK1**	**SK2**	**SK3**
Tissue homogenates							
This study	LVEF preserved; Ctl. Vs. cAF	-17% (n=14 vs. 14)	-17% (n=15 vs. 16)	+41%* (n=15 vs. 16)	-13% (n=24 vs. 18)	-1% (n=24 vs. 18)	+41% (n=21 vs. 17)
Rahm et al. Physiol Rep. 2021[57] and Life Sci. 2021	End-stage HF; Ctl. Vs. cAF	-78%** (n=10 vs. 10)	-55%** (n=10 vs. 10)	-48%* (n=10 vs. 10)			
Darkow et al. Front Physiol. 2021[18]	LVEF unknown, males only; Ctl. Vs. cAF	-29% (n=12 vs. 6)	-30%* (n=12 vs. 6)	-3% (n=12 vs. 6)			
Fan et al. Med Sci Monit. 2018[20]	LVEF preserved; Ctl. Vs. cAF	-76%* (n=20 vs. 32)	-63%* (n=20 vs. 32)	-74%* (n=20 vs. 32)	-29%* (n=20 vs. 32)	-39%* (n=20 vs. 32)	-45%* (n=20 vs. 32)
Skibsbye et al. Cardiovasc Res 2014[17]	LVEF preserved; Ctl. Vs. cAF	-19% (n=10 vs. 14)	-53%* (n=10 vs. 14)	-40%* (n=10 vs. 14)			
Ling et al. Heart Rhythm 2013	LVEF preserved; Ctl. Vs. cAF						-46%* (n=3 vs. 3)
Gaborit et al. Circ 2005	Ctl-CAD vs. cAF-VHD		-9% (n=11 vs. 11)				
Cardiomyocytes							
This study	LVEF preserved; Ctl. Vs. cAF	-38% (P=0.069; n=12 vs. 12)	-37%* (n=12 vs. 12)	+49% (n=12 vs. 12)	+32% (n=8 vs. 7)	-14% (n=13 vs. 11)	+20% (n=7 vs. 7)
Yu et al. Life Sci 2012[26]	LVEF preserved; Ctl vs. cAF	-84%* (n=8 vs. 8)	-84%** (n=8 vs. 8)	-3% (n=8 vs. 8)	-71%** (n=8 vs. 8)	-45%* (n=8 vs. 8)	-24% (n=8 vs. 8)
LA							
Reference	**Patients**	**mRNA KCNN1**	**KCNN2**	**KCNN3**	**Protein SK1**	**SK2**	**SK3**
Tissue homogenates							
This study	LVEF preserved; Ctl. Vs. cAF				+9% (n=7 vs. 5)	+30% (n=7 vs. 5)	+38% (n=7 vs. 5)
Rahm et al. Physiol Rep. 2021[57] and Life Sci. 2021	End-stage HF; Ctl. Vs. cAF	+91% (P=0.074; n=10 vs. 10)	-31% (n=10 vs. 10)	-4% (n= 10 vs. 10)			
Cardiomyocytes							
Yu et al. Life Sci 2012[26]	LVEF preserved; Ctl vs. cAF	-67%* (n=8 vs. 8)	-55%* (n=8 vs. 8)	-5% (n=8 vs. 8)	-49%* (n=8 vs. 8)	-63%* (n=8 vs. 8)	-8% (n=8 vs. 8)

Table S2. AF-related remodeling of SK-current (I_{SK}) and its role in repolarization in the current study and in the literature.

RA							
		I_{SK}			APD		
Reference	**Patients**	**[Ca^{2+}]**	**Blocker**	**Result**	**[Ca^{2+}]**	**Blocker**	**Result**
This study	LVEF preserved; Ctl. Vs. cAF	500 nmol/L 1000 nmol/L	Apamin (100 nmol/L)	500 nmol/L: +397%*[-110 mV]; +544%* [+30 mV] (n=19/12 vs. 16/10) 1000 nmol/L: +705%* [-110 mV] (n=7/4 vs. 4/3)	500 nmol/L	Apamin (100 nmol/L)	Ctl: +11% (n=8/5) cAF: +39% (n=8/6)
Yu et al. Med Sci Monit. 2020[56]	LVEF preserved; Ctl vs. cAF	500 nmol/L	Apamin (100 nmol/L)	-110 mV: +281%* +60 mV: +119%* (n=15/8 vs. 18/6)			
Shamsaldeen et al. Biochem Biophys Res Commun. 2019	LVEF preserved; mixed group (n=18), 5 with history of AF	Unknown[#]	Apamin (100 nmol/L)	+10 mV -14.3% I_M by apamin			
Fan et al. Med Sci Monit. 2018[20]	LVEF preserved; Ctl. Vs. cAF	500 nmol/L	Apamin (100 nmol/L)	-110 mV: +134%** +60 mV: +120%* (n=35/12 vs. 24/9)			
Wang et al. Zhongguo Ying Yong Sheng Li Xue Za Zhi 2014[25]	Unknown	500 nmol/L 1000 nmol/L	Apamin (100 nmol/L)	-130 mV: +134%* [500 nmol/L] (n=6 vs. 3) -130 mV: +43%* [1000 nmol/L] (n=8 vs. 4)			
Skibsbye et al. Cardiovasc Res 2014[17]	LVEF preserved; Ctl. Vs. cAF	300 nmol/L	ICAGEN (100 µmol/L)	Ctl: -28%* vs TMC (n=5 vs. n=4) cAF: -23%* vs. TMC (n=6 vs. n=3)	35 nmol/L	ICAGEN (1 µmol/L)	Ctl: +13%* vs TMC (n=7 vs. 12) cAF: -1% vs TMC (n=6 vs. 5)
Yu et al. Life Sci 2012[26]	LVEF preserved; Ctl vs. cAF	900 nmol/L	Apamin (100 nmol/L)	-120 mV: -53%* +80 mV: -55%* (n=31/18 vs. 27/14)	Perforated patch	Apamin (100 nmol/L)	Ctl: +86% (n=9/6) cAF: +10% (n=7/5)
Li et al. Zhonghua Xin Xue Guan Bing Za Zhi 2011[24]	Valve surgery patients. Details unknown	500 nmol/L	Apamin (100 nmol/L)	-130 mV: +167%* (n=15 vs. 7)			
Yu et al., Nan Fang Yi Ke Da Xue Xue Bao 2011	Congenital heart defects	1000 nmol/L	Apamin (100 nmol/L)	I_{SK} present in Ctl (n=8)	Unknown	Apamin (100 nmol/L)	Slight ↑ APD in Ctl (n=8)
LA							
		I_{SK}			AP		
Reference	**Patients**	**[Ca^{2+}]**	**Blocker**	**Result**	**[Ca^{2+}]**	**Blocker**	**Result**
Yu et al. Life Sci 2012[26]	LVEF preserved; Ctl vs. cAF	900 nmol/L	Apamin (100 nmol/L)	-120 mV: -53%* +80% -59%* (n=29/18 vs. 27/14)	Perforated patch	Apamin (100 nmol/L)	Ctl: +61% (n=9/6) cAF: +17% (n=7/5)

Patient Characteristics

Experimental protocols were approved by ethical review boards of University Hospital Essen (No. #12-5268-BO), Medical Faculty Mannheim, University of Heidelberg (No. 2011–216N-MA), and Medical Faculty, Ruhr-Universität Bochum (No. AZ 21/2013), and were conducted in accordance with the Declaration of Helsinki. Each patient provided written informed consent.

Right-atrial (RA) or left-atrial (LA) appendages were obtained from patients undergoing open heart surgery without a history of atrial fibrillation (Ctl) or with a history of long-standing persistent (chronic) atrial fibrillation (cAF). An overview of the clinical characteristics of all patients included in this study is provided in **Table S3.**

The clinical characteristics of the subsets of patients from whom samples were used for patch-clamp, PCR, Western blot or immunocytochemistry experiments are shown in **Tables S4 through S10**. Of note, 5 Ctl and 3 cAF patients undergoing open heart surgery were included for whom both RA and LA tissue samples were available for immunostaining (**Table S11**), enabling a direct comparison of SK-channel localization in both atria. Finally, a dedicated cohort of patients with preserved left-ventricular ejection-fraction (LVEF), a history of heart failure with reduced (≤35%) LVEF (HFrEF-SR) or HFrEF with cAF (HFrEF-cAF) were included to directly assess a potential modulating effect on cAF-related SK-channel remodeling. The clinical characteristics of these patients are shown in **Table S12**.

Association between clinical variables and primary outcomes

The association between clinical variables that were significantly different between Ctl and cAF cohorts and the primary outcomes (mRNA and protein levels of SK-channel subunits, their membrane localization, regulation of calmodulin, and SK-channel current) was assessed using two-way ANOVA analyses. The factors for these analyses were rhythm (Ctl vs. cAF) and either age (<72 vs. ≥72 years), sex (male vs. female), left-atrial diameter (LAD; <43 vs. ≥43 mm), presence of mitral valve insufficiency (MVI, yes/no), or diuretics use (yes/no). The threshold for age and LAD was based on their median value in the entire cohort. In addition, the potential effect of digitalis (which was present in a subset of cAF patients, but not in Ctl patients, precluding a two-way ANOVA analysis) was assessed by comparing values in cAF patients on digitalis vs. cAF patients without digitalis using Mann-Whitney tests. The significant associations are shown in **Figures S28 through S30** and the P-values of all analyses are shown in **Table S13**.

Table S3. Clinical characteristics of all patients employed in this study providing RA, LA or tissue from both atria.

	Ctl (n=182)		cAF (n=119)		P-value
	Value	N	Value	N	Value
Demographics					
Age (years)	69 (60-77)	182	74 (69-79)	119	**$1.64x10^{-4}$**
Female gender	50 (27.5%)	182	43 (36.1%)	119	0.112
BMI (kg / m^2)	27 (25-30)	163	26 (24-30)	106	0.094
Indication for surgery					
CAD AVD/MVD CAD+AVD/MVD Other	70 (39.8%) 61 (34.7%) 42 (23.9%) 3 (1.7%)	176	24 (21.2%) 64 (56.6%) 23 (20.4%) 2 (1.8%)	113	**$1.55x10^{-3}$**
Medical history					
Dyslipidemia	110 (69.2%)	159	58 (65.9%)	88	0.597
Diabetes	50 (32.1%)	156	31 (34.4%)	90	0.700
Hypertension	149 (86.6%)	172	96 (89.7%)	107	0.443
Echocardiography					
LA diameter (mm)	40.3±5.98	107	47.3±6.66	61	**$8.53x10^{-11}$**
LVEF (%)	56 (47-60)	166	58 (48-60)	102	0.901
Aortic valve insufficiency (%)	57 (54.3%)	105	37 (57.8%)	64	0.654
Mitral valve insufficiency (%)	75 (61.0%)	123	72 (83.7%)	86	**$3.96x10^{-4}$**
Medication					
ACE inhibitors or ARBs	119 (68.0%)	175	75 (67.6%)	111	0.939
Beta-blockers	118 (67.4%)	175	82 (73.9%)	111	0.247
Digitalis	2 (1.1%)	174	24 (21.6%)	111	**$4.82x10^{-9}$**
Dihydropyridines	43 (24.7%)	174	27 (24.3%)	111	0.941
Diuretics	67 (38.3%)	175	73 (65.8%)	111	**$5.89x10^{-6}$**
Lipid-lowering drugs	106 (60.6%)	175	59 (53.2%)	111	0.216
Nitrates	11 (6.3%)	174	8 (7.2%)	111	0.770

Continuous variables are presented as mean±standard deviation for normal-distributed data or median and interquartile ranges. Categorical data are provided as number of patients (%). Continuous data were compared using unpaired Student's *t*-test or Mann-Whitney test for normal and non-normal data, respectively. Categorical data were compared using Chi-squared tests. Abbreviations: ACE, angiotensin-converting enzyme; ARB, angiotensin receptor blocker; AVD/MVD, aortic/mitral valve disease; BMI, body mass index; CAD, coronary artery disease; Dihydropyridines, dihydropyridine-type Ca^{2+}-channel blockers; LA, left atrium; LVEF, left ventricular ejection fraction; N-numbers represent number of patients for which information on the corresponding clinical variable was available.

Table S4A. Clinical characteristics of all patients employed for patch-clamp recordings in this study.

	Ctl (n=50)		cAF (n=20)		P-value
	Value	N	Value	N	Value
Demographics					
Age (years)	67.6±12.0	50	73.4±6.33	20	**0.047**
Female gender	7 (14.0%)	50	9 (45.0%)	20	**0.005**
BMI (kg / m^2)	26 (25-28)	43	26 (25-27)	14	0.390
Indication for surgery					
CAD AVD/MVD CAD+AVD/MVD Other	26 (57.8%) 10 (22.2%) 8 (17.8%) 1 (2.2%)	45	7 (50.0%) 3 (21.4%) 3 (21.4%) 1 (7.1%)	14	0.812
Medical history					
Dyslipidemia	31 (79.5%)	39	6 (85.7%)	7	0.702
Diabetes	13 (33.3%)	39	2 (22.2%)	9	0.517
Hypertension	43 (97.7%)	44	11 (100.0%)	11	0.614
Echocardiography					
LA diameter (mm)	35.0 (35.0-40.5)	27	50.0 (43.5-50.0)	5	**0.019**
LVEF (%)	52.1±13.4	42	51.1±10.5	9	0.816
Aortic valve insufficiency (%)	16 (61.5%)	26	4 (80.0%)	5	0.429
Mitral valve insufficiency (%)	17 (54.8%)	31	5 (71.4%)	7	0.422
Medication					
ACE inhibitors or ARBs	35 (77.8%)	45	10 (76.9%)	13	0.948
Beta-blockers	35 (77.8%)	45	10 (76.9%)	13	0.948
Digitalis	0 (0.0%)	45	3 (23.1%)	13	**0.001**
Dihydropyridines	16 (35.6%)	45	8 (61.5%)	13	0.094
Diuretics	12 (26.7%)	45	8 (61.5%)	13	**0.020**
Lipid-lowering drugs	31 (68.9%)	45	9 (69.2%)	13	0.981
Nitrates	6 (13.3%)	45	3 (23.1%)	13	0.393

Continuous variables are presented as mean±standard deviation for normal-distributed data or median and interquartile ranges. Categorical data are provided as number of patients (%). Continuous data were compared using unpaired Student's *t*-test or Mann-Whitney test for normal and non-normal data, respectively. Categorical data were compared using Chi-squared tests. For abbreviations see **Table S3**.

Table S4B. Clinical characteristics of all patients employed for patch-clamp recordings presented in Figure 1 of this study.

	Ctl (n=12)		cAF (n=10)		P-value
	Value	N	Value	N	Value
Demographics					
Age (years)	64.0±10.5	12	74.5±6.38	10	**0.016**
Female gender	2 (16.7%)	12	7 (70.0%)	10	**0.011**
BMI (kg / m^2)	27 (26-28)	12	26 (25-27)	5	0.328
Indication for surgery					
CAD AVD/MVD CAD+AVD/MVD Other	8 (57.8%) 2 (22.2%) 2 (17.8%) 0 (2.2%)	12	1 (50.0%) 2 (21.4%) 1 (21.4%) 1 (7.1%)	5	0.196
Medical history					
Dyslipidemia	7 (63.6%)	11	2 (66.7%)	3	0.923
Diabetes	2 (16.7%)	12	0 (0.0%)	4	0.383
Hypertension	12 (100.0%)	12	5 (100.0%)	5	N/A
Echocardiography					
LA diameter (mm)	36 (35-40)	8	39 (37-41)	2	0.978
LVEF (%)	55 (45-60)	12	60 (54-60)	4	0.556
Aortic valve insufficiency (%)	5 (50.0%)	10	2 (66.7%)	3	0.612
Mitral valve insufficiency (%)	4 (44.4%)	9	3 (75.0%)	4	0.308
Medication					
ACE inhibitors or ARBs	9 (75.0%)	12	3 (60.0%)	5	0.536
Beta-blockers	9 (75.0%)	12	3 (60.0%)	5	0.536
Digitalis	0 (0.0%)	12	3 (60.0%)	5	**0.003**
Dihydropyridines	3 (25.0%)	12	3 (60.0%)	5	0.169
Diuretics	3 (25.0%)	12	2 (40.0%)	5	0.536
Lipid-lowering drugs	6 (50.0%)	12	3 (60.0%)	5	0.707
Nitrates	1 (8.3%)	12	1 (20.0%)	5	0.496

Continuous variables are presented as mean±standard deviation for normal-distributed data or median and interquartile ranges. Categorical data are provided as number of patients (%). Continuous data were compared using unpaired Student's *t*-test or Mann-Whitney test for normal and non-normal data, respectively. Categorical data were compared using Chi-squared tests. N/A: not applicable. For other abbreviations see **Table S3**.

Table S5. Clinical characteristics of all patients providing right-atrial whole-tissue homogenates employed for qPCR experiments in this study.

	Ctl (n=15)		cAF (n=16)		P-value
	Value	N	Value	N	Value
Demographics					
Age (years)	69.1±8.42	15	76.0±6.87	16	**0.022**
Female gender	3 (20.0%)	15	4 (25.0%)	16	0.739
BMI (kg / m^2)	28.0±4.81	15	25.9±3.68	16	0.201
Indication for surgery					
CAD AVD/MVD CAD+AVD/MVD Other	5 (33.3%) 3 (20.0%) 7 (46.7%) 0 (0%)	15	4 (25.0%) 10 (62.5%) 2 (12.5%) 0 (0.0%)	16	**0.010**
Medical history					
Dyslipidemia	10 (66.7%)	15	8 (50.0%)	16	0.347
Diabetes	7 (50.0%)	14	7 (43.8%)	16	0.732
Hypertension	11 (73.3%)	15	16 (100.0%)	16	**0.027**
Echocardiography					
LA diameter (mm)	36 (35-39)	4	48 (48-48)	5	**0.032**
LVEF (%)	55 (45-60)	14	60 (58-63)	15	0.100
Aortic valve insufficiency (%)	5 (100.0%)	5	6 (100.0%)	6	N/A
Mitral valve insufficiency (%)	4 (66.7%)	6	7 (100.0%)	7	0.097
Medication					
ACE inhibitors or ARBs	5 (33.3%)	15	7 (43.8%)	16	0.552
Beta-blockers	9 (60.0%)	15	12 (75.0%)	16	0.372
Digitalis	0 (0.0%)	15	4 (25.0%)	16	**0.038**
Dihydropyridines	2 (13.3%)	15	5 (31.3%)	16	0.233
Diuretics	3 (20.0%)	15	12 (75.0%)	16	**0.002**
Lipid-lowering drugs	9 (60.0%)	15	11 (68.8%)	16	0.611
Nitrates	0 (0.0%)	15	0 (0.0%)	16	N/A

Continuous variables are presented as mean±standard deviation for normal-distributed data or median and interquartile ranges. Categorical data are provided as number of patients (%). Continuous data were compared using unpaired Student's *t*-test or Mann-Whitney test for normal and non-normal data, respectively. Categorical data were compared using Chi-squared tests. N/A: not applicable. For other abbreviations see **Table S3**.

Table S6. Clinical characteristics of all patients providing right-atrial whole-tissue homogenates employed for Western blot experiments in this study.

	Ctl (n=60)		cAF (n=46)		P-value
	Value	N	Value	N	Value
Demographics					
Age (years)	70 (60-77)	45	71 (64-76)	30	0.741
Female gender	12 (26.7%)	45	10 (33.3%)	30	0.534
BMI (kg / m^2)	28 (26-32)	40	27 (25-30)	27	0.283
Indication for surgery					
CAD AVD/MVD CAD+AVD/MVD Other	19 (42.2%) 17 (37.8%) 9 (20.0%) 0 (0.0%)	45	5 (16.7%) 19 (63.3%) 5 (16.7%) 1 (3.3%)	30	0.052
Medical history					
Dyslipidemia	27 (65.9%)	41	19 (73.1%)	26	0.535
Diabetes	13 (31.7%)	41	7 (30.4%)	23	0.916
Hypertension	40 (88.9%)	45	27 (93.1%)	29	0.545
Echocardiography					
LA diameter (mm)	41.2±5.94	22	46.9±9.49	13	**0.043**
LVEF (%)	55 (50-64)	42	59 (50-60)	29	0.669
Aortic valve insufficiency (%)	16 (57.1%)	28	7 (36.8%)	19	0.172
Mitral valve insufficiency (%)	14 (48.3%)	29	21 (87.5%)	24	**0.003**
Medication					
ACE inhibitors or ARBs	30 (69.8%)	43	22 (73.3%)	30	0.741
Beta-blockers	27 (62.8%)	43	23 (76.7%)	30	0.209
Digitalis	1 (2.3%)	43	6 (20.0%)	30	**0.012**
Dihydropyridines	13 (30.2%)	43	4 (13.3%)	30	0.093
Diuretics	18 (41.9%)	43	17 (56.7%)	30	0.213
Lipid-lowering drugs	22 (51.2%)	43	16 (53.3%)	30	0.855
Nitrates	4 (9.3%)	43	4 (13.3%)	30	0.588

Continuous variables are presented as mean±standard deviation for normal-distributed data or median and interquartile ranges. Categorical data are provided as number of patients (%). Continuous data were compared using unpaired Student's *t*-test or Mann-Whitney test for normal and non-normal data, respectively. Categorical data were compared using Chi-squared tests. For abbreviations see **Table S3**.

Table S7. Clinical characteristics of all patients providing right-atrial cardiomyocytes employed for digital PCR experiments in this study.

	Ctl (n=12)		cAF (n=12)		P-value
	Value	N	Value	N	Value
Demographics					
Age (years)	65.8±8.48	12	73.3±7.25	12	**0.037**
Female gender	2 (16.7%)	12	3 (25.0%)	12	0.615
BMI (kg / m^2)	27 (26-29)	12	26 (24-29)	12	0.453
Indication for surgery					
CAD AVD/MVD CAD+AVD/MVD Other	6 (50.0%) 4 (33.3%) 2 (16.7%) 0 (0.0%)	12	3 (25.0%) 7 (58.3%) 2 (16.7%) 0 (0%)	12	0.403
Medical history					
Dyslipidemia	10 (100.0%)	10	3 (100.0%)	3	N/A
Diabetes	2 (28.6%)	7	1 (100.0%)	1	0.168
Hypertension	11 (100.0%)	11	10 (100.0%)	10	N/A
Echocardiography					
LA diameter (mm)	41.69±7.69	9	45.22±5.53	9	0.307
LVEF (%)	54.18±6.09	11	53.45±8.14	11	0.823
Aortic valve insufficiency (%)	4 (100.0%)	4	3 (100.0%)	3	N/A
Mitral valve insufficiency (%)	9 (100.0%)	9	9 (100.0%)	9	N/A
Medication					
ACE inhibitors or ARBs	10 (83.3%)	12	10 (83.3%)	12	1.000
Beta-blockers	7 (58.3%)	12	11 (91.7%)	12	0.059
Digitalis	0 (0.0%)	12	0 (0.0%)	12	N/A
Dihydropyridines	4 (33.3%)	12	2 (16.7%)	12	0.346
Diuretics	4 (33.3%)	12	9 (75.0%)	12	**0.041**
Lipid-lowering drugs	9 (75.0%)	12	5 (41.7%)	12	0.098
Nitrates	0 (0.0%)	12	0 (0.0%)	12	N/A

Continuous variables are presented as mean±standard deviation for normal-distributed data or median and interquartile ranges. Categorical data are provided as number of patients (%). Continuous data were compared using unpaired Student's *t*-test or Mann-Whitney test for normal and non-normal data, respectively. Categorical data were compared using Chi-squared tests. N/A: not applicable. For other abbreviations see **Table S3**.

Table S8. Clinical characteristics of all patients providing right-atrial cardiomyocytes employed for Western blot experiments in this study.

	Ctl (n=27)		cAF (n=28)		P-value
	Value	N	Value	N	Value
Demographics					
Age (years)	66.7±13.1	15	70.5±11.8	16	0.423
Female gender	7 (46.7%)	15	10 (62.5%)	16	0.376
BMI (kg / m^2)	27 (23-28)	15	26 (24-28)	16	0.945
Indication for surgery					
CAD AVD/MVD CAD+AVD/MVD Other	5 (33.3%) 10 (66.7%) 0 (0.0%) 0 (0.0%)	15	0 (0.0%) 9 (56.3%) 7 (43.8%) 0 (0.0%)	16	**0.002**
Medical history					
Dyslipidemia	7 (53.8%)	13	6 (50.0%)	12	0.848
Diabetes	3 (20.0%)	15	6 (37.5%)	16	0.283
Hypertension	13 (86.7%)	15	13 (81.3%)	16	0.682
Echocardiography					
LA diameter (mm)	42.80±5.83	10	46.75±4.12	8	0.146
LVEF (%)	58.36±9.08	14	55.93±8.94	15	0.491
Aortic valve insufficiency (%)	4 (26.7%)	15	6 (54.5%)	11	0.149
Mitral valve insufficiency (%)	9 (64.3%)	14	14 (87.5%)	16	0.134
Medication					
ACE inhibitors or ARBs	10 (66.7%)	15	11 (73.3%)	15	0.690
Beta-blockers	9 (60.0%)	15	11 (73.3%)	15	0.439
Digitalis	0 (0.0%)	15	6 (40.0%)	15	**0.006**
Dihydropyridines	1 (6.7%)	15	2 (13.3%)	15	0.543
Diuretics	4 (26.7%)	15	7 (46.7%)	15	0.256
Lipid-lowering drugs	6 (40.0%)	15	4 (26.7%)	15	0.439
Nitrates	1 (6.7%)	15	1 (6.7%)	15	1.000

Continuous variables are presented as mean±standard deviation for normal-distributed data or median and interquartile ranges. Categorical data are provided as number of patients (%). Continuous data were compared using unpaired Student's *t*-test or Mann-Whitney test for normal and non-normal data, respectively. Categorical data were compared using Chi-squared tests. For abbreviations see **Table S3**.

Table S9. Clinical characteristics of all patients providing right-atrial cardiomyocytes employed for immunocytochemistry experiments in this study.

	Ctl (n=13)		cAF (n=12)		P-value
	Value	N	Value	N	Value
Demographics					
Age (years)	64 (59-72)	13	77 (74-80)	12	**0.018**
Female gender	6 (46.2%)	13	2 (16.7%)	12	0.114
BMI (kg / m^2)	27.5±4.05	13	27.6±3.50	11	0.966
Indication for surgery					
CAD AVD/MVD CAD+AVD/MVD Other	3 (23.1%) 3 (23.1%) 6 (46.2%) 1 (7.7%)	13	4 (33.3%) 5 (41.7%) 3 (25.0%) 0 (0%)	12	0.456
Medical history					
Dyslipidemia	10 (76.9%)	13	10 (90.9%)	11	0.360
Diabetes	6 (50.0%)	12	4 (36.4%)	11	0.510
Hypertension	12 (92.3%)	13	11 (100.0%)	11	0.347
Echocardiography					
LA diameter (mm)	39 (35-45)	9	49 (45-50)	5	0.072
LVEF (%)	60 (59-60)	11	60 (60-60)	9	0.676
Aortic valve insufficiency (%)	2 (40.0%)	5	2 (50.0%)	4	0.764
Mitral valve insufficiency (%)	8 (88.9%)	9	5 (83.3%)	6	0.756
Medication					
ACE inhibitors or ARBs	8 (61.5%)	13	7 (58.3%)	12	0.870
Beta-blockers	9 (69.2%)	13	8 (66.7%)	12	0.891
Digitalis	1 (7.7%)	13	2 (16.7%)	12	0.490
Dihydropyridines	1 (7.7%)	13	4 (33.3%)	12	0.109
Diuretics	6 (46.2%)	13	10 (83.3%)	12	0.053
Lipid-lowering drugs	10 (76.9%)	13	10 (83.3%)	12	0.689
Nitrates	0 (0.0%)	13	0 (0.0%)	12	N/A

Continuous variables are presented as mean±standard deviation for normal-distributed data or median and interquartile ranges. Categorical data are provided as number of patients (%). Continuous data were compared using unpaired Student's *t*-test or Mann-Whitney test for normal and non-normal data, respectively. Categorical data were compared using Chi-squared tests. N/A: not applicable. For other abbreviations see **Table S3**.

Table S10. Clinical characteristics of all patients providing left-atrial whole-tissue homogenates employed for Western blot experiments in this study.

	Ctl (n=7)		cAF (n=6)		P-value
	Value	N	Value	N	Value
Demographics					
Age (years)	81 (76-84)	7	82 (81-83)	6	0.807
Female gender	4 (57.1%)	7	4 (66.7%)	6	0.725
BMI (kg / m^2)	25 (24-29)	7	25 (23-26)	6	0.432
Indication for surgery					
CAD AVD/MVD CAD+AVD/MVD Other	0 (0.0%) 2 (28.6%) 5 (71.4%) 0 (0.0%)	7	0 (0.0%) 5 (83.3%) 1 (16.7%) 0 (0.0%)	6	**0.048**
Medical history					
Dyslipidemia	3 (42.9%)	7	3 (50.0%)	6	0.797
Diabetes	2 (28.6%)	7	1 (16.7%)	6	0.612
Hypertension	4 (57.1%)	7	4 (66.7%)	6	0.725
Echocardiography					
LA diameter (mm)	43 (42-44)	6	48 (46-55)	6	**0.024**
LVEF (%)	59 (57-61)	7	59 (56-60)	6	0.812
Aortic valve insufficiency (%)	2 (28.6%)	7	3 (50.0%)	6	0.429
Mitral valve insufficiency (%)	3 (42.9%)	7	5 (83.3%)	6	0.135
Medication					
ACE inhibitors or ARBs	4 (57.1%)	7	4 (66.7%)	6	0.725
Beta-blockers	3 (42.9%)	7	5 (83.3%)	6	0.135
Digitalis	0 (0.0%)	7	2 (33.3%)	6	0.097
Dihydropyridines	3 (42.9%)	7	1 (16.7%)	6	0.308
Diuretics	5 (71.4%)	7	5 (83.3%)	6	0.612
Lipid-lowering drugs	2 (28.6%)	7	2 (33.3%)	6	0.853
Nitrates	0 (0.0%)	7	0 (0.0%)	6	N/A

Continuous variables are presented as mean±standard deviation for normal-distributed data or median and interquartile ranges. Categorical data are provided as number of patients (%). Continuous data were compared using unpaired Student's *t*-test or Mann-Whitney test for normal and non-normal data, respectively. Categorical data were compared using Chi-squared tests. N/A not applicable. For other abbreviations see **Table S3**.

Table S11. Clinical characteristics of all patients providing paired right- and left-atrial tissue slices employed for immunocytochemistry in this study.

	Ctl (n=5)		cAF (n=3)		P-value
	Value	N	Value	N	Value
Demographics					
Age (years)	74 (72-79)	5	71 (70-76)	3	0.786
Female gender	1 (20.0%)	5	1 (33.3%)	3	0.673
BMI (kg / m^2)	29 (25-29)	5	28 (26-30)	3	0.786
Indication for surgery					
CAD	1 (20.0%)	5	0 (0.0%)	3	0.641
AVD/MVD	2 (40.0%)		2 (66.7%)		
CAD+AVD/MVD	2 (40.0%)		1 (33.3%)		
Other	0 (0.0%)		0 (0.0%)		
Medical history					
Dyslipidemia	1 (20.0%)	5	2 (66.7%)	3	0.187
Diabetes	1 (20.0%)	5	0 (0.0%)	3	0.408
Hypertension	2 (40.0%)	5	2 (66.7%)	3	0.465
Echocardiography					
LA diameter (mm)	43 (42-43)	5	46 (46-53)	3	0.125
LVEF (%)	59 (52-61)	5	57 (49-62)	3	0.875
Aortic valve insufficiency (%)	3 (60.0%)	5	2 (66.7%)	3	0.850
Mitral valve insufficiency (%)	2 (40.0%)	5	1 (33.3%)	3	0.850
Medication					
ACE inhibitors or ARBs	2 (40.0%)	5	1 (33.3%)	3	0.850
Beta-blockers	3 (60.0%)	5	2 (66.7%)	3	0.850
Digitalis	0 (0.0%)	5	0 (0.0%)	3	N/A
Dihydropyridines	1 (20.0%)	5	0 (0.0%)	3	0.408
Diuretics	4 (80.0%)	5	1 (33.3%)	3	0.187
Lipid-lowering drugs	2 (40.0%)	5	1 (33.3%)	3	0.850
Nitrates	0 (0.0%)	5	0 (0.0%)	3	N/A

Continuous variables are presented as mean±standard deviation for normal-distributed data or median and interquartile ranges. Categorical data are provided as number of patients (%). Continuous data were compared using unpaired Student's *t*-test or Mann-Whitney test for normal and non-normal data, respectively. Categorical data were compared using Chi-squared tests. N/A not applicable. For other abbreviations see **Table S3**.

Table S12. Clinical characteristics of all patients providing right-atrial whole-tissue homogenates employed for the heart failure sub-study.

	Ctl (n=11)		HFrEF-SR (n=12)		HFrEF-cAF (n=8)		P-value
	Value	N	Value	N	Value	N	Value
Demographics							
Age (years)	69.4±7.80	11	62.6±12.2	12	72.0±6.16	8	0.102
Female gender	6 (54.5%)	11	3 (25.0%)	12	2 (25.0%)	8	0.259
BMI (kg / m^2)	26 (25-33)	9	28 (26-34)	6	28 (23-32)	6	0.903
Indication for surgery							
CAD AVD/MVD CAD+AVD/MVD Other	2 (18.2%) 8 (72.7%) 1 (9.1%) 0 (0.0%)	11	4 (36.4%) 3 (27.3%) 3 (27.3%) 1 (9.1%)	11	1 (12.5%) 7 (87.5%) 0 (0.0%) 0 (0.0%)	8	0.166
Medical history							
Dyslipidemia	6 (60.0%)	10	6 (66.7%)	9	2 (28.6%)	7	0.280
Diabetes	3 (27.3%)	11	1 (14.3%)	7	3 (37.5%)	8	0.599
Hypertension	8 (72.7%)	11	6 (66.7%)	9	4 (50.0%)	8	0.584
Echocardiography							
LA diameter (mm)	37.75±3.70	8	42.67±3.94	9	46.63±5.72	8	**0.005**
LVEF (%)	65 (61-68)	11	35 (32-35)	12	32 (29-35)	8	**0.001**
Aortic valve insufficiency (%)	5 (55.6%)	9	1 (33.3%)	3	4 (57.1%)	7	0.765
Mitral valve insufficiency (%)	2 (33.3%)	6	4 (80.0%)	5	5 (62.5%)	8	0.279
Medication							
ACE inhibitors or ARBs	8 (72.7%)	11	8 (66.7%)	12	4 (57.1%)	7	0.792
Beta-blockers	7 (63.6%)	11	11 (91.7%)	12	4 (57.1%)	7	0.171
Digitalis	0 (0.0%)	11	0 (0.0%)	11	1 (14.3%)	7	0.196
Dihydropyridines	2 (18.2%)	11	1 (9.1%)	11	0 (0.0%)	7	0.460
Diuretics	5 (45.5%)	11	8 (66.7%)	12	4 (57.1%)	7	0.591
Lipid-lowering drugs	8 (72.7%)	11	7 (58.3%)	12	3 (42.9%)	7	0.446
Nitrates	0 (0.0%)	11	0 (0.0%)	11	0 (0.0%)	7	N/A

Continuous variables are presented as mean±standard deviation for normal-distributed data or median and interquartile ranges. Categorical data are provided as number of patients (%). Continuous data were compared using one-way ANOVA or Kruskal-Wallis test for normal and non-normal data, respectively. Categorical data were compared using Chi-squared tests. N/A not applicable. For other abbreviations see **Table S3**.

Table S13. Association between clinical variables and primary outcomes.

Parameter	Source	Clinical variable					
		Age	Sex	LAD	MVI	Diuretic	Digitalis
KCNN1 mRNA	RA homogenates (**Figure S12**)	0.62	0.110	0.440	N/A	0.630	0.374
KCNN2 mRNA		0.712	0.731	0.672	N/A	0.722	0.170
KCNN3 mRNA		0.573	0.302	0.255	N/A	0.262	0.953
KCNN1 mRNA	RA cardiomyocytes (**Figure S14**)	0.444	0.273	0.672	N/A	0.035	N/A
KCNN2 mRNA		0.720	0.740	0.192	N/A	0.931	N/A
KCNN3 mRNA		0.518	0.984	0.649	N/A	0.847	N/A
SK1 protein	RA homogenates (**Figure S13**)	0.704	0.783	0.042	0.127	0.469	0.270
SK2 protein		0.760	0.476	0.090	0.767	0.767	0.929
SK3 protein		0.600	0.110	0.600	0.011	0.123	0.664
SK1 protein	LA homogenates (**Figure S13**)	N/A	0.628	N/A	N/A	0.869	0.999
SK2 protein		N/A	0.670	N/A	N/A	0.744	0.999
SK3 protein		N/A	0.288	N/A	N/A	0.0043	0.200
SK1 protein	RA cardiomyocytes (**Figure 2C**)	0.645	0.467	0.182	0.517	0.682	0.229
SK2 protein		0.913	0.027	0.262	0.488	0.362	0.778
SK3 protein		0.899	0.194	0.031	0.957	0.228	0.229
SK2 mem / cyt	RA tissue slices (**Figure 3**)	0.302	0.395	N/A	0.495	0.052	N/A
SK3 mem / cyt		0.242	0.687	N/A	0.559	0.311	N/A
SK2 mem / cyt	LA tissue slices (**Figure 3**)	0.617	0.476	N/A	0.215	0.291	N/A
SK3 mem / cyt		0.138	0.302	N/A	0.316	0.633	N/A
SK1 mem / cyt	RA cardiomyocytes (**Figure 4**; **Figure S19**	N/A	0.822	N/A	N/A	0.597	N/A
SK2 mem / cyt		N/A	0.713	N/A	N/A	0.530	N/A
SK3 mem / cyt		N/A	0.614	N/A	N/A	0.999	0.122
PP2Ac	LA homogenates (**Figure S22**)	N/A	0.389	N/A	N/A	0.728	0.800
PP2Ac	RA cardiomyocytes (**Figure 6D**)	0.563	0.799	0.519	0.503	0.724	0.012
CaM-Total	RA homogenates (**Figure S21**)	0.762	0.848	0.782	0.387	0.495	0.234
CaM-Thr80-P/Total		0.373	0.505	0.400	0.275	0.343	0.731
CaM-Total	LA homogenates (**Figure S22**)	N/A	0.710	N/A	N/A	0.940	0.200
CaM-Thr80-P/Total		N/A	0.286	N/A	N/A	0.644	0.200
CaM-Total	RA cardiomyocytes (**Figure 6C**)	0.505	0.509	0.707	0.590	0.107	0.935
CaM-Thr80-P/Total		0.328	0.174	0.082	0.857	0.891	0.683
ISK (+30 mV) - Per Patient	RA cardiomyocytes (**Figure 1D**)	0.432	0.654	N/A	N/A	0.799	0.999
Apamin-induced APD prolongation	RA cardiomyocytes (**Figure 1F**)	0.542	N/A	N/A	N/A	N/A	0.473

P-values for two-way ANOVA analyses with factors rhythm status (Ctl vs. cAF) and either age (<72 vs. ≥72 years), sex (male vs. female), left-atrial diameter (LAD; <43 vs. ≥43 mm), mitral valve insufficiency (MVI; yes/no), or diuretics use (no vs. yes) are shown for mRNA and protein levels of SK-channel subunits, their membrane localization, regulators of calmodulin, and SK-channel current (I_{SK}). P-values for digitalis are based on Mann-Whitney tests between cAF patients on

digitalis compared to cAF patients without digitalis. P-values are not corrected for multiple comparisons and results should be considered hypothesis generating. P=N/A indicates the inability to perform two-way ANOVA because there are not enough patients in one of the four combinations of rhythm and clinical status. The statistically significant associations are highlighted in orange and are shown in **Figures S28 through S30**.

Experimental Methods

Whole-cell patch-clamp recordings

Standard patch-clamp recording techniques were used to measure currents in the whole-cell configuration. Patch electrodes were pulled from borosilicate glass capillaries (MTW 150F; world Precision Instruments, Inc., Sarasota, FL) using a DMZ-Universal Puller (Zeitz-Instrumente Vertriebs GmbH, Martinsried, Germany) and filled with pre-filtered pipette solution. Currents or action potentials (APs) were recorded at room temperature with an EPC-8 amplifier (HEKA Elektronik, Lambrecht, Germany) connected via a 16 bit A/D interface to a computer. The signals were low-pass filtered (1 kHz) before 5 kHz digitization. Data acquisition and analysis were performed with an ISO-3 multitasking patch-clamp program (MFK M. Friedrich, Niedernhausen, Germany). Pipette resistance ranged from 2-3 MΩ. Electrode offset potentials were always zero-adjusted before a GΩ-seal was formed. After a GΩ-seal was obtained, the membrane under the pipette tip was ruptured by negative pressure and the whole-cell configuration was established. In voltage-clamp but not in current-clamp recordings, the membrane capacitance and series resistance were compensated (60-80%).

Whole-cell currents were elicited by applying 300-ms step pulses to potentials ranging from -120 mV to +80 mV in 10-mV increments from a holding potential of -50 mV. The whole-cell currents were measured at the end of each pulse, normalized to cell capacitance to obtain the current density (pA/pF) and plotted versus the respective voltages, yielding the activation (I/V) curves of channels in the cell. APs were elicited in current-clamp mode with a holding current of -40 pA by injection of brief current pulses (2 ms, 1 nA). In a subset of experiments, stable currents or APs were first recorded with the aforementioned protocols at 0.2 Hz (baseline). Then, the patched cells were stimulated in voltage-clamp mode by AP-like pulses at 5 Hz for 10 mins. Thereafter, the stimulation protocol was changed back to the control protocol at 0.2 Hz and currents or APs were recorded with the same protocol at the same frequency (0.2 Hz) as in baseline recordings to eliminate any direct effects of frequency on channel gating.

In whole-cell current measurements and AP recordings, the bath was superfused with (in mmol/L): 130 NaCl, 5.9 KCl, 2.4 $CaCl_2$, 1.2 $MgCl_2$, 11 glucose, 10 HEPES, pH 7.4 with NaOH. The pipette solution contained (in mmol/L) 126 KCl, 6 NaCl, 1.2 $MgCl_2$, 5 EGTA, 11 glucose, 1 MgATP, 0.1 Na3GTP, and 10 HEPES adjusted to pH 7.4 with KOH, free-Ca^{2+} 500 nmol/L.

Quantitative real-time or digital polymerase chain reaction

Total RNA was isolated from RA appendages or RA cardiomyocytes from Ctl and cAF patients using the RNeasy Mini Kit (Qiagen, Hilden, Germany) according to the manufacturer's instructions, after disrupting the tissue with the tissue lyser LT (Qiagen, Hilden, Germany). Subsequently, the mRNA in 1 µg of total RNA was transcribed into cDNA using the reverse transcription kit (Applied Biosystems; Thermo Fisher Scientific, Waltham, MA) according to the manufacturer's instructions. Quantitative polymerase chain reaction was performed with TaqMan probes and primers from Applied Biosystems; Thermo Fisher Scientific for *KCNN1* (Hs00158457_m1), *KCNN2* (Hs00222059_m1), and *KCNN3* (Hs01546821_m1), as well as the

housekeeping genes hydroxymethylbilane synthase (*HMBS*; Hs00609296_g1), beta-2-microglobulin (*B2M*, Hs99999907_m1) and GATA binding protein 4 (*GATA4*; Hs00171403_m1). Reactions were run on a Pikoreal 96 (Thermo Fisher Scientific, Waltham, MA) using the following conditions: 2 minutes at 50°C, followed by 10 minutes at 95°C, a total of 45 cycles (15 sec at 95°C and 1 minute at 60°C), and 30 sec at 60°C. Relative gene expression values were calculated by the 2^DCt method as described.[30]

Alternatively, 140 ng RNA was transcribed into cDNA using the reverse transcription kit (Applied Biosystems; Thermo Fisher Scientific, Waltham, MA) according to the manufacturer's instructions. Digital polymerase chain reaction (dPCR) was carried out with TaqMan probes from Thermo Fisher Scientific for KCNN1 (Hs01109326_m1), KCNN2 (Hs00222059_m1), and KCNN3 (Hs01546821_m1) and the aforementioned primers for the housekeeping genes HBMS, B2M and GATA4. cDNA dilution of 1:1 was used for KCNN1, KCNN2, KCNN3, HBMS, as well GATA4 and 1:10 for B2M. The reactions were run on a QIAcuity Digital PCR System (Qiagen, Hilden, Germany) using a 96-well Nanoplate with 8500 partitions and the QIAcuity master mix according to the manufacturer's instructions. The cycling program used for the reactions consisted of 2 minutes at 50°C, followed by 10 minutes at 95°C, a total of 35 cycles (15 seconds at 95°C and 1 minute at 60°C), and 30 sec at 60°C. The relative mRNA levels to controls were calculated from the copies/µl values and normalized to HMBS, B2M and GATA.

Co-immunoprecipitation and immunoblot

Human RA or LA whole-tissue lysates or human RA cardiomyocyte fractions were subjected to electrophoresis on acrylamide gels, followed by transfer onto polyvinyl difluoride (PVDF) membranes. Co-immunoprecipitation and immunoblotting were performed according to standard procedures, as described,[31-33] using the primary antibodies listed in the **Major Resources Table**. Appropriate peroxidase-conjugated (1:20,000, Santa-Cruz Biotechnology, Dallas, TX, or Merck Sigma-Aldrich, Darmstadt, Germany) or near-infrared fluorophore dyes (IRDye, all 1:20,000, LI-COR Biosciences, Lincoln, NE) were employed as secondary antibodies and imaged with a ChemoCam Imager (Intas Science Imaging Instruments, Göttingen, Germany) or an Odyssey Infrared Imaging System (LI-COR Biosciences). Protein expression was normalized to GAPDH for whole-tissue homogenates or to troponin-C for cardiomyocytes.

Immunostaining

Human atrial tissue slices

Human LA and RA appendages from Ctl or cAF patients were snap frozen and stored in liquid nitrogen until further use. Prior to sectioning, the tissue was placed in Tissue-Tek® medium (Sakara Fintek, Alphen aan den Rijn, The Netherlands) and sectioned in 10 µm thick slices on a cryostat setup (Leica CM3050S, Leica Microsystems, Wetzlar, Germany). Cryosections were air-dried for 30 min and rehydrated for 10 min in 1x phosphate-buffered saline (PBS) before they were fixed in 4% paraformaldehyde (PFA) for 20 min. The sections were then blocked with 2% bovine serum albumin (BSA) and 2.2% glycine in 1xPBS and incubated at 4°C overnight in blocking buffer with the primary rabbit polyclonal SK2 (APC-028, 1:200) or SK3 (APC-039, 1:200)

antibodies (Alomone, Jerusalem, Israel) and conjugated Wheat Germ Agglutinin (WGA)-AF350 (Invitrogen, W11263, 1:500) to visualize the cellular membrane. Thereafter, the sections were washed in 1xPBS and incubated for 1 hour at room temperature with secondary antibody Cy5 (111-175-144, Jackson ImmunoResearch, West Grove, PA, 1:200). After washing with 1xPBS, the sections were mounted on coverslips with aqueous mounting medium (Abcam, ab128982). The slices were imaged using Keyence BZ-X800E at 40x magnification and 2-6 frames per section were acquired.

For analyses, the images were imported in Fiji (www.fiji.sc), an extended version of ImageJ. Only transversely sectioned cardiomyocytes with intact membrane morphology within a given frame were chosen for analysis. Partial or incomplete cardiomyocytes were not included in the analysis. The membrane regions and the cytosolic regions of each cell selected for analysis were traced based on the WGA staining (**Figure S16**). Thereafter, the mean membrane intensity and the mean cytosolic intensity of the SK2 and SK3 signal was analyzed based on these regions (**Figure S16**). Results are shown in **Figure 3**. Background staining was assessed in human atrial tissue slices by incubation with the secondary antibody in absence of the primary antibody. Subsequent imaging did not reveal any unspecific background staining, as shown for a representative example in **Figure S16B**.

Human atrial cardiomyocytes

For immunostaining of RA cardiomyocytes (**Figure 4**; **Figure S19**), cells were fixed with 2% PFA for 15 min in a 15 ml plastic tube. After centrifugation for 5 min at 700 rpm, PFA was removed and the myocytes were washed and PFA was neutralized with Glycine 0.1 mol/L for 10 min. Cells were washed 3 times with PBS and permeabilized with Triton X-100 diluted in PBS (0.2%, 15 min). Cells were rinsed 3 times with PBS and blocked with a PBS solution containing 1% BSA for 40 min. Double-labelling was obtained by incubating the myocytes overnight at 4°C with the primary antibodies diluted in PBS containing 10% goat serum and 0.25% Triton X-100: mouse monoclonal anti-α-actinin (1:1000 dilution) and rabbit polyclonal SK1 (APC-039, 1:200 dilution), SK2 (APC-028, 1:200 dilution), or SK3 (APC-025, 1:200 dilution). Cardiomyocytes were subsequently rinsed 3 times with 1% BSA in PBS (5 min). The cells were then incubated with AlexaFluor® 488 conjugate anti-rabbit IgG to reveal SK channels and AlexaFluor® 633 anti-mouse IgG to reveal the α-actinin. After 3 successive washes with PBS/BSA for 5 min and centrifugation (700 rpm, 5 min), the cells were resuspended in Mowiol mounting medium (15 µL), placed on a slide and carefully covered with a coverslip avoiding air bubbles. The coverslip was then secured on the slide with nail polish and examined with a Carl Zeiss (Oberkochen, Germany) LSM 710 confocal scanning laser microscope. Optical sections series were obtained with a Plan Apochromat 63x objective (NA 1.4, oil immersion). Background staining in human atrial cardiomyocytes was assessed using only the secondary antibody.

For immunostaining of RA cardiomyocytes after electrical field stimulation (**Figure 8**; **Figure S27**), circular coverslips (11 mm) were laminin coated (20µg/ml in water, 90 min at room temperature) in 6-well cell culture plates and washed 3 times with bath solution containing (in mmol/L): NaCl 140, HEPES 10, KCl 4, $MgCl_2$ 1, $CaCl_2$ 2, glucose 10. Freshly isolated human RA cardiomyocytes from Ctl patients were allowed to settle for 1 hour on the coverslips supplied with 150 µl bath

solution each. Subsequently, 3 ml bath solution was added per well and the cells were field stimulated at 0.2 Hz or 5 Hz (C-Pace EM & C-Dish, 6-well corning; Ionoptix) for 10 minutes and fixed immediately after stimulation with 3.7% PFA. After removal of PFA and washing (3x PBS), cardiomyocytes were permeabilized with 0.1 % Triton X-100 in PBS for 10 minutes. After further washing steps (3x PBS), cardiomyocytes were blocked with 10% Roti-Block (Roth) in PBS and incubated with 1:250 diluted primary antibodies in PBS (SK1: APC-039, Alomone; SK2: APC-028, Alomone; SK3: APC-025, Alomone; Alpha-Actinin: A7811, Sigma) over night at 4°C. Coverslips were then washed 3x with PBS+0.2% Tween20 (PBST) and incubated with FITC- and Cy5-coupled secondary antibodies (11-4614-80, Thermo Fisher; and SBA-1031-15, Dianova Biozol, respectively) diluted 1:250 in PBS for 2 hours at room temperature and washed again 3 times with PBST and 1 time with PBS. The sample coverslips were supplied with 5.5µl mounting medium (ab104139, Abcam), placed on glass slides and insulated with nail polish. The fluorescence signals of individual cells in FITC-, Cy5- and DAPI-channel as well as a brightfield cell image was acquired using a epifluorescence (BZ-X810, Keyence) or a Carl Zeiss (Oberkochen, Germany) LSM 710 confocal scanning laser microscope.

Computational Modeling

We developed updated computational models of Ctl and cAF human atrial cardiomyocytes based on the framework of the Grandi et al. model,[34] previously modified to reproduce Na^+-dependent regulation of I_{K1} and $I_{K,Ach}$.[35] Here, we integrated into this cellular framework a previously published model of I_{K2P}[36] and a novel formulation of I_{SK}.

Mathematical model of I_{SK}

The new I_{SK} formulation was based on published data and our new experimental data collected in this study. In our cellular model, the total I_{SK} current is the sum of two components, one carried by SK channels located in the junctional space (junc) and one carried by SK channels located in the subsarcolemmal space (sl):

$$I_{SK} = I_{SK,junc} + I_{SK,sl}$$

Each component is calculated multiplying the fraction of SK channels in each compartment (F_{junc} = 0.11; F_{sl} = 0.89), the maximal conductance G_{SK}, a function describing the Ca^{2+}-dependent activation (F_{Ca}), a function integrating voltage-dependent properties (F_{Vm}), and the driving force (i.e., the difference between the voltage potential V_m and the Nernst potential for K^+ ions E_K):

$$I_{SK,junc} = F_{junc} * G_{SK} * F_{Ca,junc} * F_{Vm} * (V_m-E_K)$$
$$I_{SK,sl} = F_{sl} * G_{SK} * F_{Ca,sl} * F_{Vm} * (V_m-E_K)$$

F_{Vm}, common to both components, is calculated as follows:

$$F_{Vm} = 0.273/(1+\exp((V_m-E_K+2.964)*0.2))+0.279/(1+\exp((-(V_m-E_K-86.929)*6.363e-3)));$$

F_{Ca} depends on the local Ca^{2+} concentration in each compartment ($[Ca^{2+}]_{junc}$ and $[Ca^{2+}]_{sl}$):

$$F_{Ca,junc} = 1/(1+\exp((\log10(K_{d,SK})-\log10([Ca^{2+}]_{junc}))/0.3));$$
$$F_{Ca,sl} = 1/(1+\exp((\log10(K_{d,SK})-\log10([Ca^{2+}]_{sl}))/0.3));$$

where the SK apparent affinity for Ca^{2+} ($K_{d,SK}$) was set to 355 nmol/L, in agreement with published observations in rabbit and rat ventricular cardiomyocytes[63,64] and dog atrial cardiomyocytes.[7] The SK maximal conductance (G_{SK}) and gating parameters were fitted to reproduce the I_{SK}-voltage relationships experimentally observed in human Ctl and cAF myocytes with $[Ca^{2+}]_i$ clamped to 500 nmol/L (**Figure S4**). Note that G_{SK} is the only parameter that changes between the Ctl and cAF I_{SK} parameterizations (G_{SK} = 0.051 mS/µF in Ctl and G_{SK} = 0.265 mS/µF in cAF). All other parameters are unchanged.

Other model parameter adjustments

After including the I_{K2P} and I_{SK} formulations, we made the following adjustments to the nSR and cAF cellular models:

- the conductance of the fast Na^+ current was increased by 15% to increase the maximal upstroke velocity in both Ctl and cAF models;

- the late Na^+ current was added to the Ctl model;
- the conductance of the background Cl^- current was reduced by 25% in Ctl & cAF models;
- the extent of cAF-induced remodeling on the transient-outward and the ultrarapid delayed-rectifier K^+ currents (I_{to} and I_{Kur}) was modified to match experimental data.[65]

Moreover, we made the following modifications to reproduce higher diastolic Ca^{2+} in cAF vs nSR, with no changes in the sarcoplasmic reticulum Ca^{2+} loading:[39,66]

- the conductance of the background Ca^{2+} current (I_{CaB}) was increased by 50% in the cAF vs Ctl model;
- the maximal SERCA transport rate was decreased by 25% in cAF vs Ctl;
- the SERCA *Kmf* was increased by 25% in cAF vs Ctl (i.e., SERCA affinity for cytosolic Ca^{2+} was reduced in cAF vs Ctl);
- the parameter *ec50SR* was increased by 25% to increase the RyR sensitivity to luminal Ca^{2+} in cAF vs Ctl.

Global parameter optimization

The parameters of the updated whole-cell model were fitted using a parameter optimization routine[67] to recapitulate experimentally observed data describing frequency-dependence of AP and Ca^{2+}-transient properties measured in Ctl and cAF human myocytes, and prolongation induced by complete block of I_{SK} (with $[Ca^{2+}]_i$ clamped to 500 nM) or I_{K2P} at 0.2 Hz. The routine uses the Nelder-Mead algorithm to minimize the error function comparing simulated and experimental outcomes, and determines the optimal combination of parameter scaling factors for the Ctl and cAF cellular models (**Figure S5**). Targets of model optimizations are reported in **Table S14**, while the resulting scaling factors are shown in **Table S15**.

Model validation

The Ctl and cAF models were validated against an independent data set describing the degree of AP shortening induced by nifedipine administration at different pacing rates[68] (**Figure S9**). Nifedipine administration was simulated by reducing the maximal conductance of the L-type Ca^{2+} channel by 50%.

Analysis

The optimized Ctl and cAF models were used to assess the consequences of I_{SK} block at different pacing rates while simulating physiologic oscillations in cytosolic Ca^{2+}. Parameter sensitivity analysis was performed using an established population-based approach[37] to assess the influence of small variations in several model parameters (including G_{SK} and $K_{d,SK}$) on model outcomes. Briefly, we generated two populations of 1000 Ctl and cAF myocytes by randomly varying the parameters indicated in **Table S15**. For each trial, the baseline value of each parameter was independently varied with a log-normal distribution ($\sigma = 0.1$), and model outputs were assessed after 300-s pacing at 1 Hz. When creating a population with $\sigma = 0.1$, 95% of

perturbed parameters are within 82 to 122% of the value present in the baseline model. Multivariable regression (non-linear iterative partial least squares method) on log-transformed values was used to correlate the variation in each parameter to the consequent effect on APD_{50}, APD_{90} and RMP in the two populations of Ctl and cAF models. In particular, a regression coefficient can be used to predict the value of each AP feature in response to a known perturbation in the baseline value of the model parameter. For example, $APD_{90} = APD_{90,baseline} * x^b$; where b is the value of the regression coefficient, $APD_{90,baseline}$ is the value of the feature estimated in the baseline model, and x is the scaling factor that describes the change in the parameter with respect to the baseline value (e.g., $G_{to} = x*G_{to,baseline}$).

Table S14. Targets of global optimization routine.

	Target	Value	Notes
APD (absolute values)			
1	APD_{90} Ctl @ 0.2 Hz	260 ms	Estimated from different papers (see **Figure S6**)
2	APD_{90} Ctl @ 3 Hz	180 ms	
3	APD_{90} cAF @ 0.2 Hz	120 ms	
4	APD_{90} cAF @ 3 Hz	90 ms	
ΔAPD (relative prolongation induced by channel block)			
5	ΔAPD_{90} Ctl @ 0.2 Hz with I_{K2P} block	17.10%	Schmidt et al. 2015[36]
6	ΔAPD_{90} cAF @ 0.2 Hz with I_{K2P} block	57%	
7	ΔAPD_{90} Ctl @ 0.2 Hz with I_{SK} block (w/ Ca^{2+} clamped to 500 nM)	11.10%	New data
8	ΔAPD_{90} cAF @ 0.2 Hz with I_{SK} block (w/ Ca^{2+} clamped to 500 nM)	47.80%	
Ca^{2+} handling properties			
9	CaT_{amp} Ctl @ 0.5 Hz	>220 nM	Voigt et al. 2012[39]
10	CaT_{amp} cAF @ 0.5 Hz	>100 nM	
11	CaT_{min} Ctl @ 0.5 Hz	>160 nM	Neef et al. 2010[66], Voigt et al. 2012[39]
12	CaT_{min} cAF @ 0.5 Hz	>200 nM	
13	$[Ca^{2+}]_{SR,max}$ Ctl @ 0.5 Hz	0.4-0.5 mM	Neef et al. 2010[66]
14	$[Ca^{2+}]_{SR,max}$ cAF @ 0.5 Hz	>0.4 mM	
Relative contributions to Ca^{2+} removal from the cytosol			
15	SERCA-to-NCX ratio Ctl @ 0.5 Hz	2.64	Voigt et al. 2012[39]
16	SERCA-to-NCX ratio cAF @ 0.5 Hz	1.02	
Other constrains			
17	RMP Ctl @ 0.5 Hz – RMP cAF @ 0.5 Hz	>4 mV	These additional constrains are needed to avoid unrealistic results
18	RMP Ctl @ 3 Hz – RMP cAF @ 3 Hz	>2 mV	
19	dV/dt_{max} Ctl @ 0.5 Hz	200-240 mV/ms	
20	$[Na^+]_i$ Ctl @ 3 Hz	<14 mM	
21	CaT_{amp} Ctl @ 0.5 Hz / CaT_{amp} Ctl @ 0.2 Hz	>1.1	

Table S15. Results of global optimization routine.

	Parameter	Definition	Lower boundary	Upper boundary	Scaling factor
1	$gNa^{\#}$	Fast Na^+ current, conductance	0.9	1	0.999
2	$gNaL^{\#}$	Late Na^+ current, conductance	0.9	1.1	0.991
3	$gNaB^{\#}$	Background Na^+ current, conductance	0.9	1.1	0.996
4	$vNaK^{\#}$	Na^+/K^+ ATPase, rate	0.9	1.1	0.901
5	$Gto^{\#}$	Transient-outward K^+ current, conductance	0.33	3	1.935
6	$GKr^{\#}$	Rapidly activating delayed-rectifier K^+ current, conductance	0.33	3	0.822
7	$GKs^{\#}$	Slowly activating delayed-rectifier K^+ current, conductance	0.33	3	0.402
8	$gKur^{\#}$	Ultrarapid delayed-rectifier K^+ current, conductance	0.33	3	0.560
9	$GK1+GK,ACh,c^{\#}$	Total inward-rectifier K^+ current, conductance (comprising basal I_{K1} and constitutively-active $I_{K,ACh,c}$)	0.33	3	1.084
10	$GKp^{\#}$	Plateau K^+ current, conductance	0.33	3	0.492
11	$GK2P^{\#}$	Two-pore-domain K^+ current, conductance	0.33	3	1.730
12	$GSK^{\#}$	Small-conductance Ca^{2+}-activated K^+ current, conductance	0.33	3	0.460
13	$KdSK^{\#}$	Small-conductance Ca^{2+}-activated K^+ current, Ca^{2+}-affinity	0.75	1.25	0.794
14	$gClCa^{\#}$	Ca^{2+}-activated Cl^- current, conductance	0.5	1.5	0.505
15	$GClB^{\#}$	Background Cl^- current, conductance	0.5	2	1.788
16	$gCaL^{\#}$	L-type Ca^{2+} current, conductance	0.5	1.5	1.475
17	$GCaB^{\#}$	Background Ca^{2+} current, conductance	0.5	1	0.998
18	$vPMCA^{\#}$	Plasma membrane Ca^{2+} ATPase, rate	0.5	1.5	0.572
19	$vNCX^{\#}$	Na^+/Ca^{2+} exchanger, rate	0.5	1.5	1.215
20	$vSERCA^{\#}$	Sarcoplasmic reticulum Ca^{2+} ATPase, rate	0.5	1.5	0.894
21	Kmf	Sarcoplasmic reticulum Ca^{2+} ATPase, Ca^{2+}-affinity	0.5	1.25	0.907
22	$vRel^{\#}$	Ryanodine receptor flux, rate	0.5	1.5	0.967
23	$vLeak^{\#}$	Ryanodine receptor Ca^{2+} leak, rate	0.5	1.5	0.726
24	$GK2P_{(cAF\ vs\ nSR)}$	cAF-to-nSR ratio in GK2P	0.5	2	1.892

25	$GSK_{(cAF\ vs\ nSR)}$	cAF-to-nSR ratio in GSK	0.5	2	1.053
26	$GCaB_{(cAF\ vs\ nSR)}$	cAF-to-nSR ratio in GCaB	0	3	2.919
27	$vNCX_{(cAF\ vs\ nSR)}$	cAF-to-nSR ratio in vNCX	0.75	2	0.986
28	$koCa_{(cAF\ vs\ nSR)}$	cAF-to-nSR ratio in koCa, parameter controlling ryanodine receptor gating	0.25	2	0.290
29	$vSERCA_{(cAF\ vs\ nSR)}$	cAF-to-nSR ratio in vSERCA	0	2	0.195
30	$Kmf_{(cAF\ vs\ nSR)}$	cAF-to-nSR ratio in Kmf	0	2	1.482
31	$ec50SR_{(cAF\ vs\ nSR)}$	cAF-to-nSR ratio in ec50SR, parameter controlling ryanodine receptor gating	0	2	0.670
32	$GK1_{(cAF\ vs\ nSR)}$	cAF-to-nSR ratio in GK1	0.5	1.5	1.468

# indicates parameters perturbed to create the populations of models (i.e., parameters 1-20, 22 and 23).

Supplemental Figures

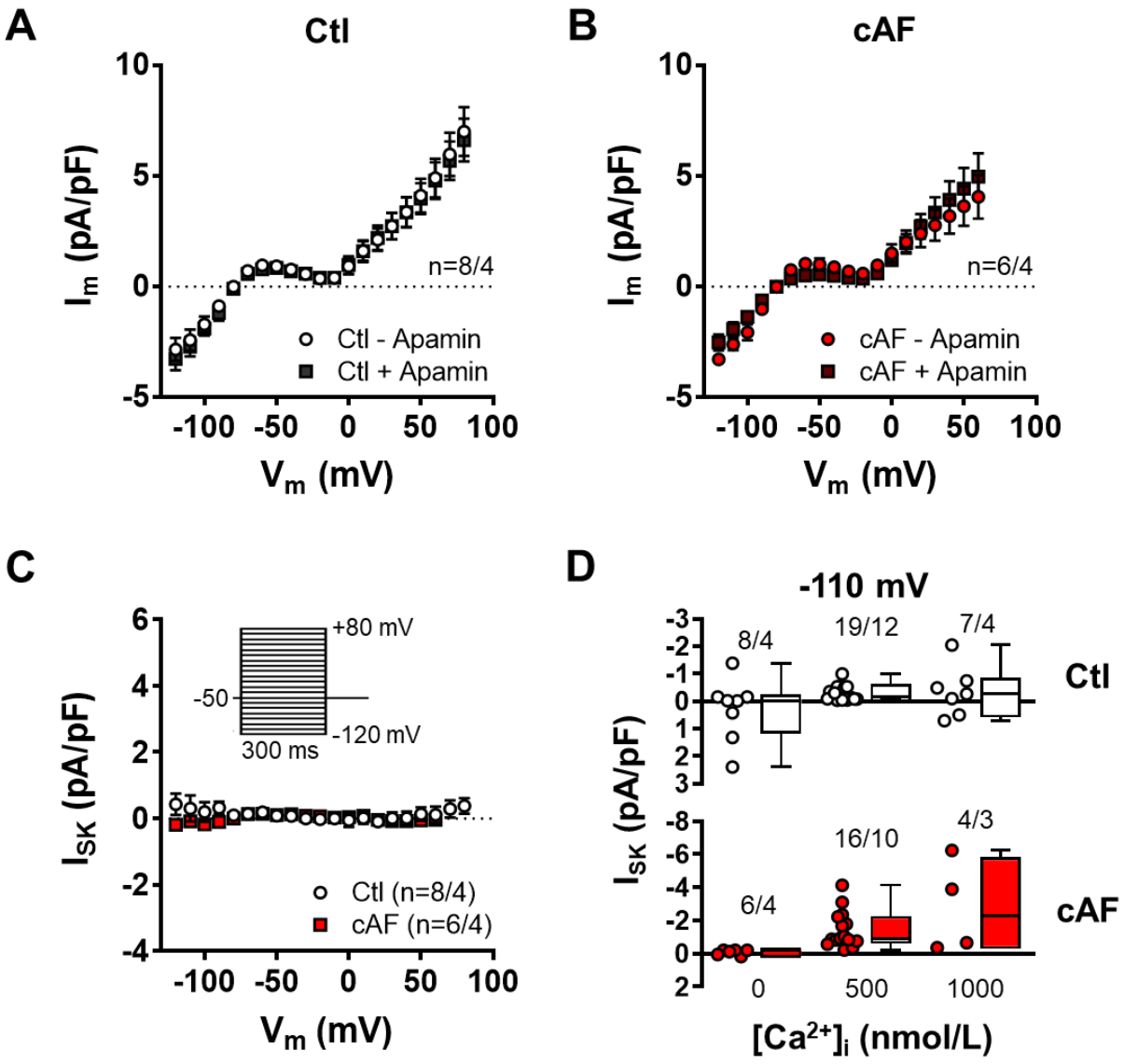

Figure S1. Ca^{2+} dependence of small-conductance Ca^{2+}-activated K^+-current (I_{SK}). A-B, Total membrane current during 300-ms voltage-clamp steps to potentials from -120 mV to +80 mV in right-atrial (RA) Ctl- or cAF-cardiomyocytes in the absence (circles) or presence (black squares) of 100-nmol/L apamin in the presence of BAPTA-AM to chelate all free Ca^{2+}. **C,** Apamin-sensitive I_{SK} in Ctl (white symbols) or cAF (red symbols) RA-cardiomyocytes in the absence of intracellular $[Ca^{2+}]$. D, Apamin-sensitive I_{SK} at -110 mV in Ctl (top) or cAF (bottom) RA-cardiomyocytes in the presence of 0-nmol/L (data from panel **C**), 500-nmol/L (data from **Figure 1**) or 1000 nmol/L free Ca^{2+}. N-numbers indicate numbers of cardiomyocytes/patients.

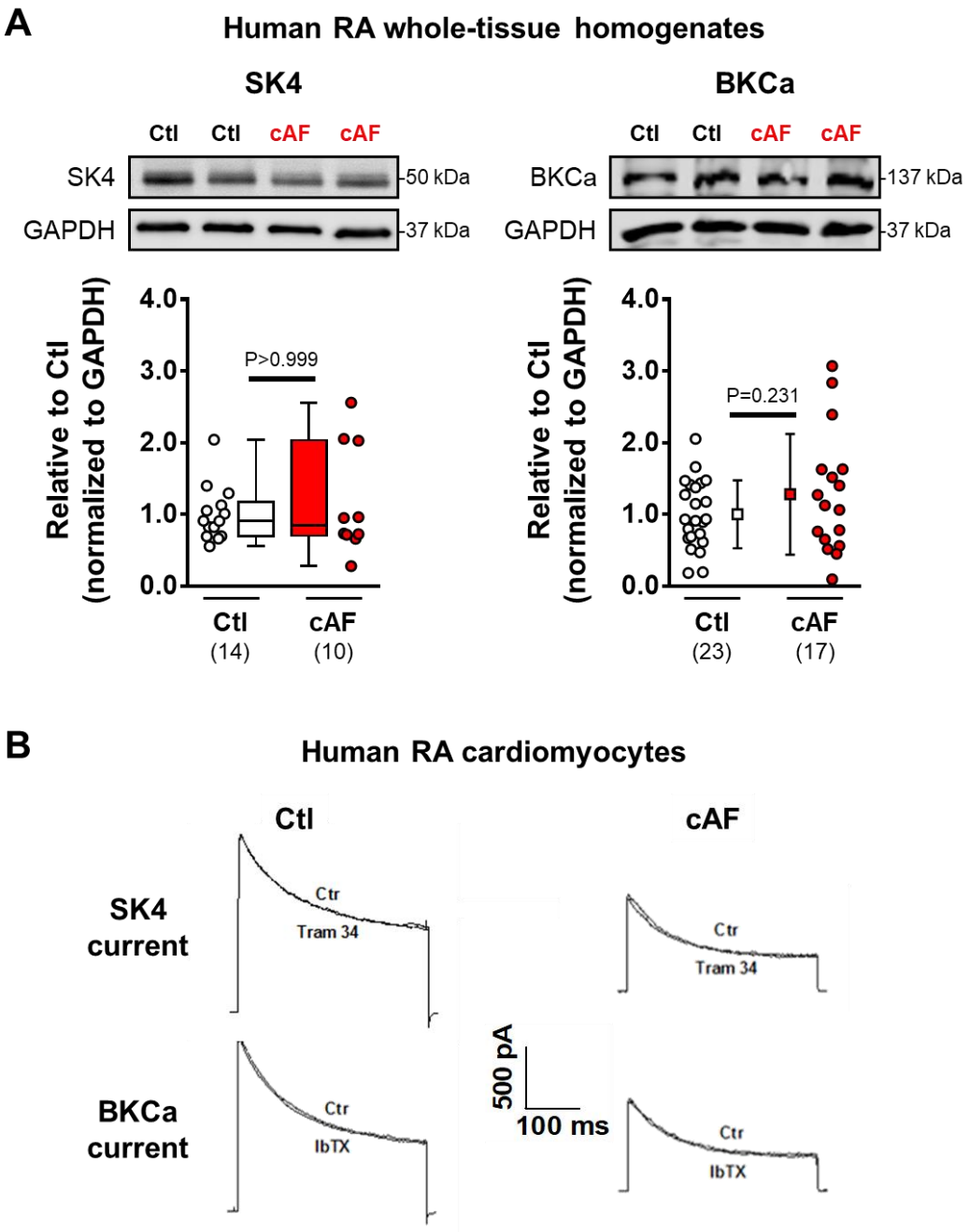

Figure S2. Intermediate and big-conductance Ca^{2+}-activated K^+-currents (SK4 and BKCa, respectively) in Ctl- and cAF-patients. A, Example Western blots (**top**) and protein levels (**bottom**) of SK4 (**left** panels) and BKCa (**right** panels) channel subunits in right-atrial (RA) whole-tissue homogenates of Ctl- and cAF-patients. GAPDH was used as loading control. **B,** Membrane-current recordings during a 300-ms depolarization pulse to +80 mV in Ctl (**left**) or cAF (**right**) human RA-cardiomyocytes in the absence and presence of the SK4-current blocker Tram34 (100-nmol/L, **top**) or the BKCa-current blocker iberiotoxin (ibTX, 300-nmol/L, **bottom**), indicating the absence of functional SK4 or BKCa channels. N-numbers indicate number of patients. P-values are based on Mann-Whitney test (SK4) or unpaired Student's *t*-test (BKCa).

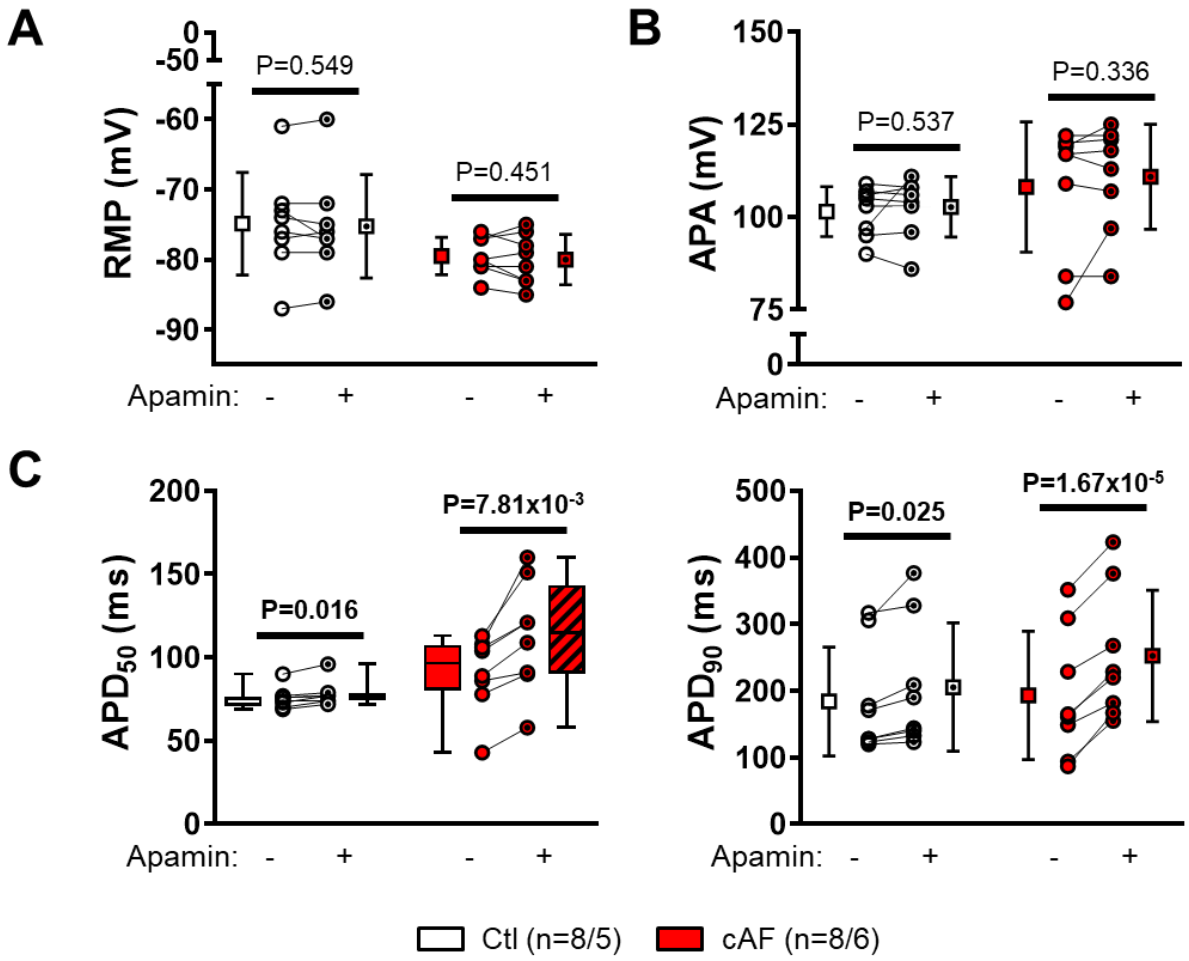

Figure S3. Apamin-induced changes in action potential (AP) characteristics. A-C, Resting membrane potential (RMP; **A**), AP amplitude (APA; **B**) and AP duration at 50% or 90% of repolarization (APD_{50} and APD_{90}, **C**) before and after application of apamin (100-nmol/L) in right-atrial cardiomyocytes from Ctl- and cAF-patients. N-numbers indicate numbers of cardiomyocytes/patients. P-values are based on paired Student's *t*-test (for RMP, APA and APD_{90}) or Wilcoxon signed rank test for paired samples (for APD_{50}) before and after apamin application.

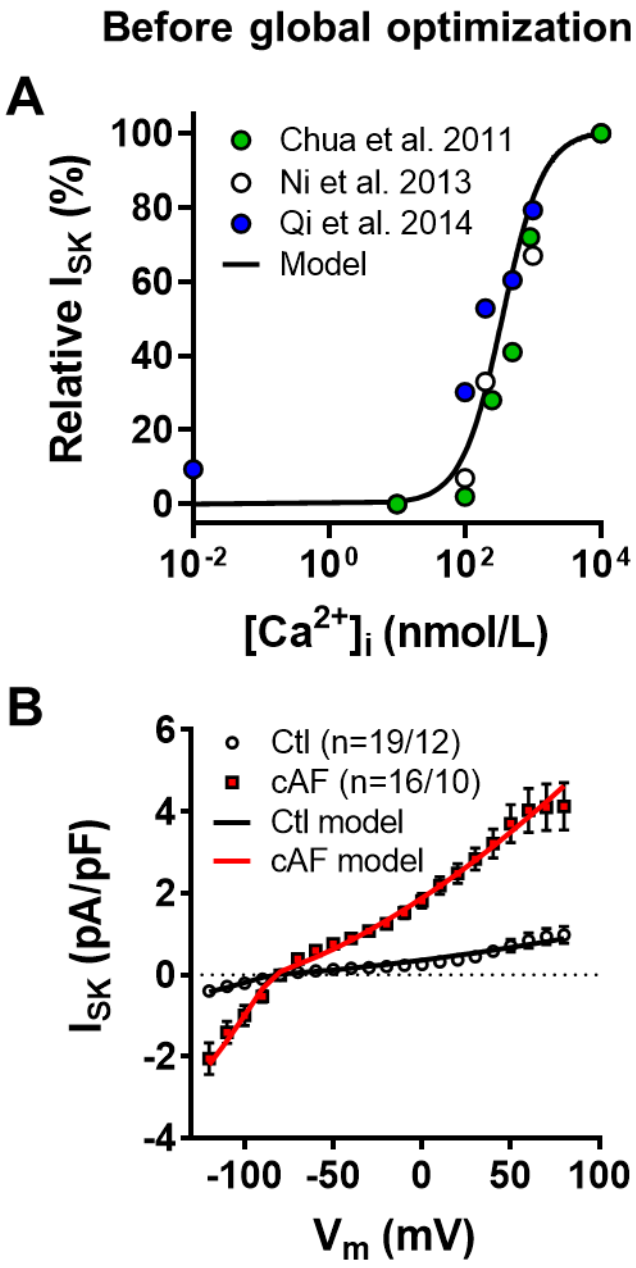

Figure S4. Small-conductance Ca^{2+}-activated K^+ current (I_{SK}) formulation. A, Experimental[7,63,64] and simulated Ca^{2+} dependence of I_{SK}. **B,** Experimental and simulated voltage dependence of I_{SK} in Ctl and cAF human atrial cardiomyocytes (with intracellular Ca^{2+} buffered at 500 nmol/L).

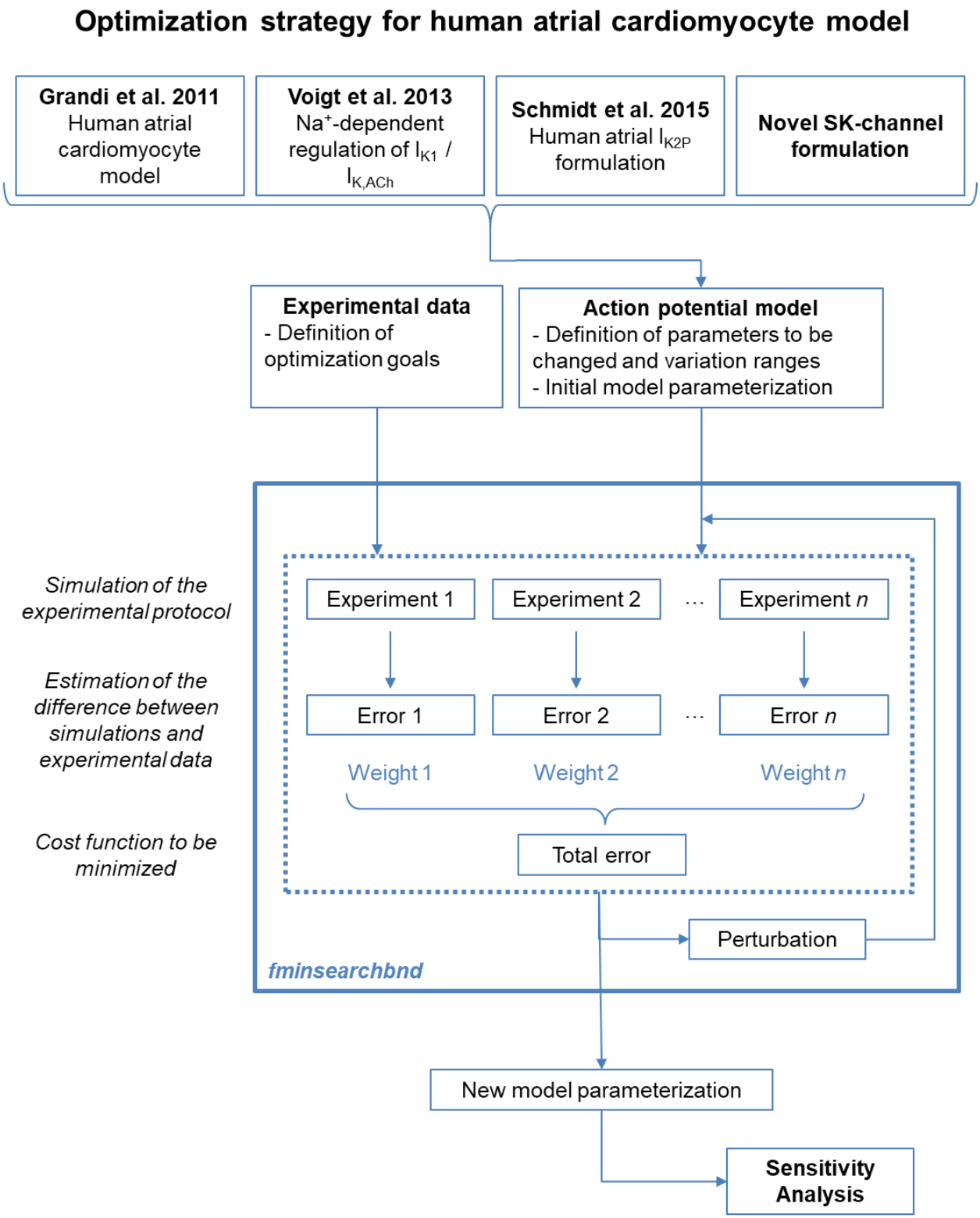

Figure S5. Flow chart showing the methodology adopted for building and optimizing the Ctl and cAF versions of the human atrial cardiomyocyte model.

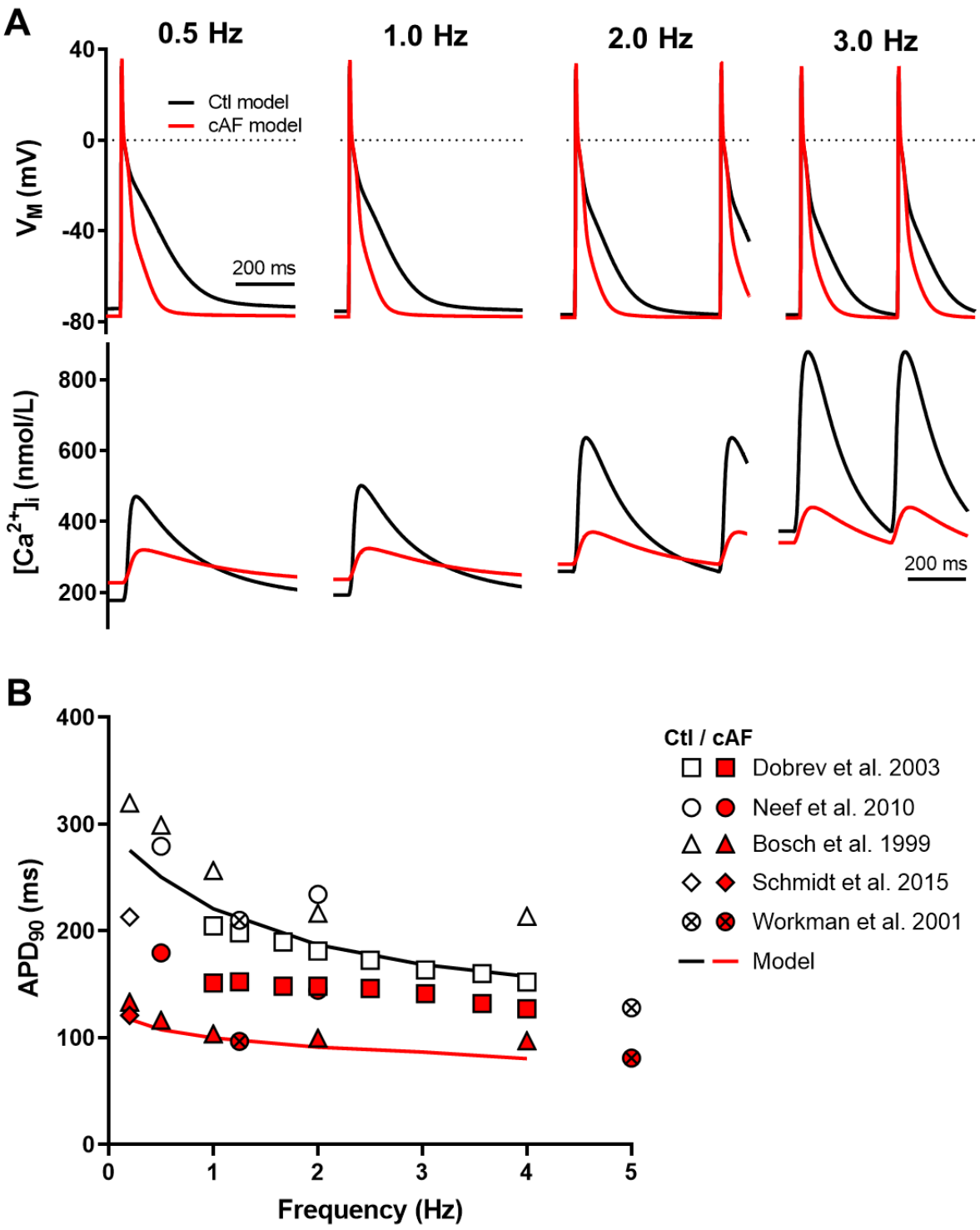

Figure S6. Frequency dependence of action potential duration (APD). A, Simulated time courses of membrane potential and cytosolic Ca^{2+} transient obtained during steady-state pacing of the Ctl and cAF models at pacing rates of 0.5, 1, 2 and 3 Hz. **B,** Experimental[36,59,66,69,70] and simulated rate-dependence of APD_{90} values in Ctl and cAF human atrial cardiomyocytes.

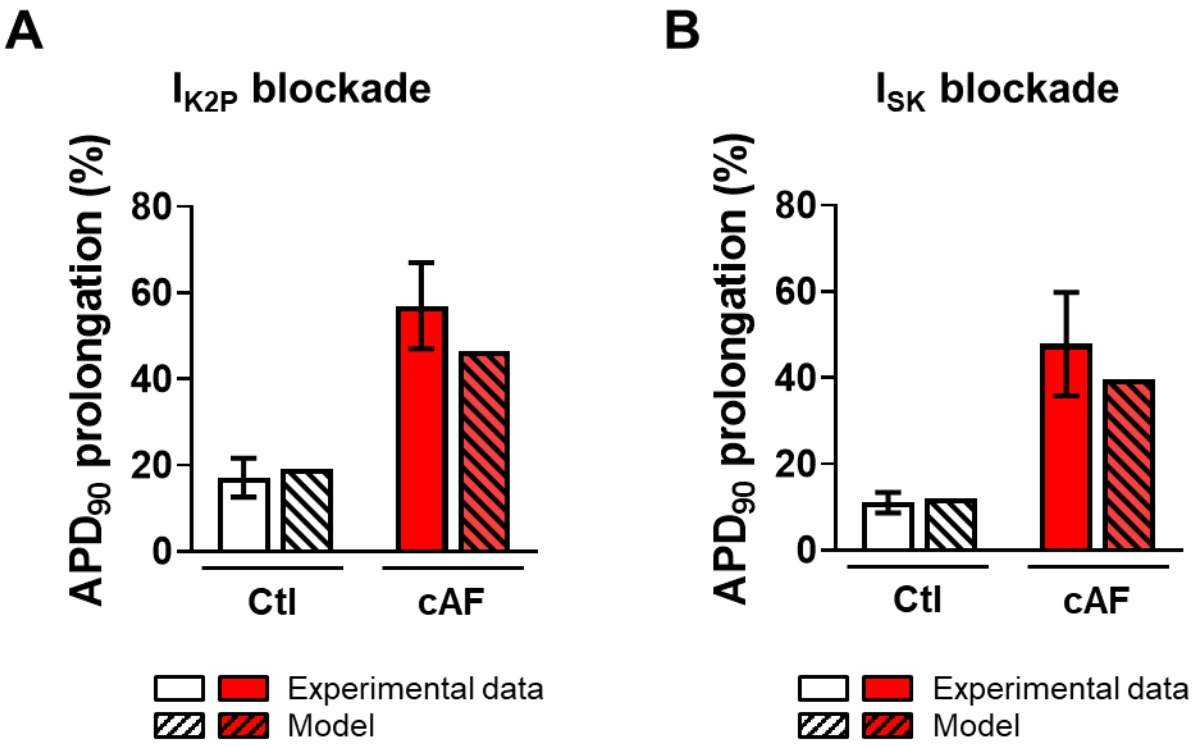

Figure S7. Consequences of two-pore domain K^+ current (I_{K2P}) and small-conductance Ca^{2+}-activated K^+ current (I_{SK}) block. A, Relative prolongation of action potential duration (APD_{90}) induced by selective I_{K2P} block in Ctl and cAF human atrial cardiomyocytes in experiments[36] and simulations. **B,** Relative APD_{90} prolongation induced by selective I_{SK} block in Ctl and cAF human atrial cardiomyocytes (with internal Ca^{2+} buffered at 500 nmol/L) in experiments (data from **Figure 1**) and simulations.

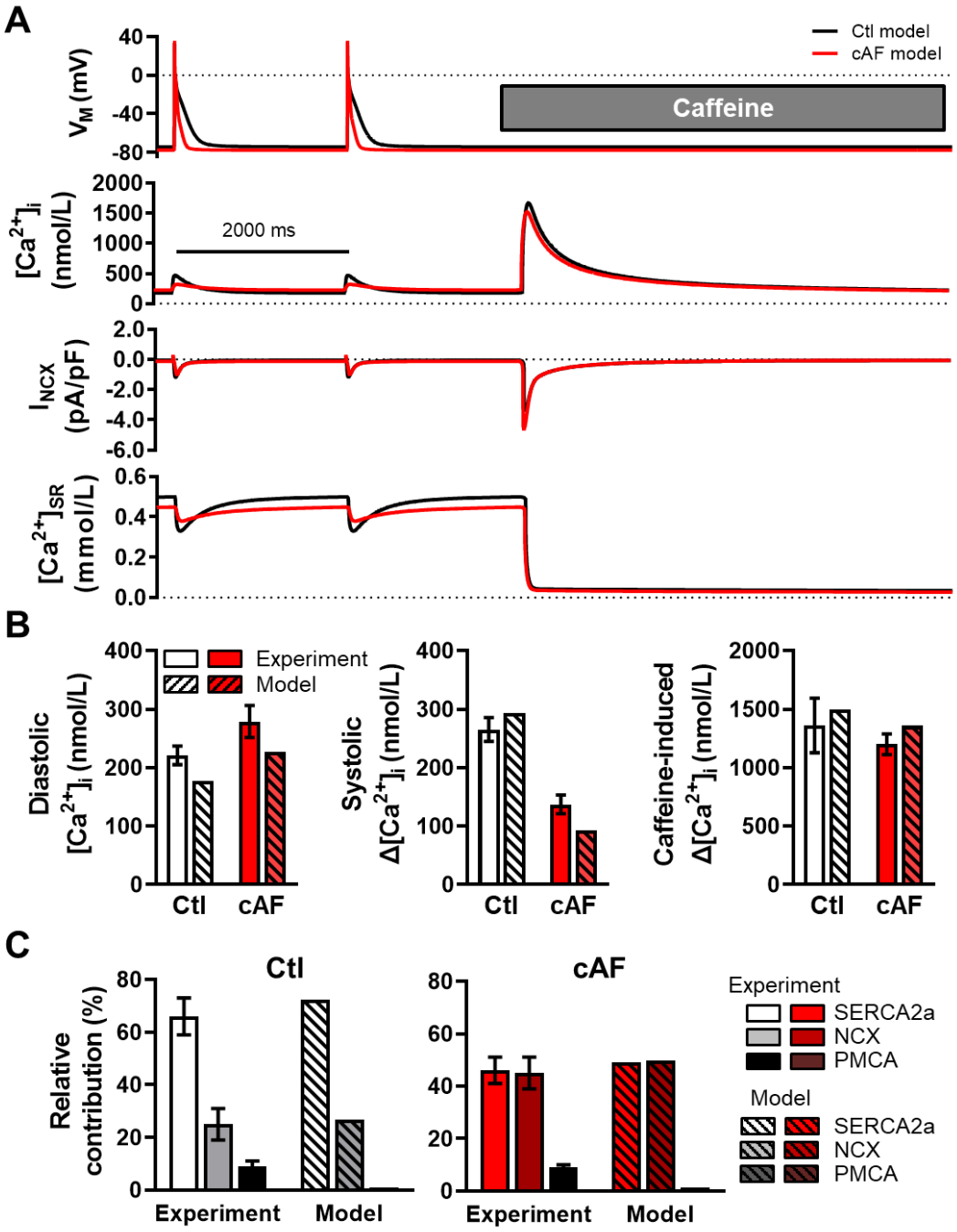

Figure S8. Characterization of Ca^{2+} handling properties. A, Time course of membrane potential (V_M), cytosolic Ca^{2+} concentration ($[Ca^{2+}]_i$), Na^+/Ca^{2+}-exchanger current (I_{NCX}), and sarcoplasmic reticulum Ca^{2+} load ($[Ca^{2+}]_{SR}$) during two action potentials at 0.5-Hz pacing and simulated application of caffeine. **B,** Comparison of diastolic $[Ca^{2+}]_i$ (**left**), systolic Ca^{2+}-transient amplitude (middle) and amplitude of the caffeine-induced Ca^{2+} transient (**right**) in Ctl and cAF human atrial cardiomyocytes[39] and models. **C,** Relative contributions to total cytosolic Ca^{2+} removal of sarcoplasmic reticulum Ca^{2+} ATPase (SERCA), Na^+/Ca^{2+} exchanger (NCX), and plasma membrane Ca^{2+} ATPase (PMCA) assessed during 0.5-Hz pacing in Ctl (**left**) and cAF (**right**) cardiomyocytes in experiments[39] and simulations.

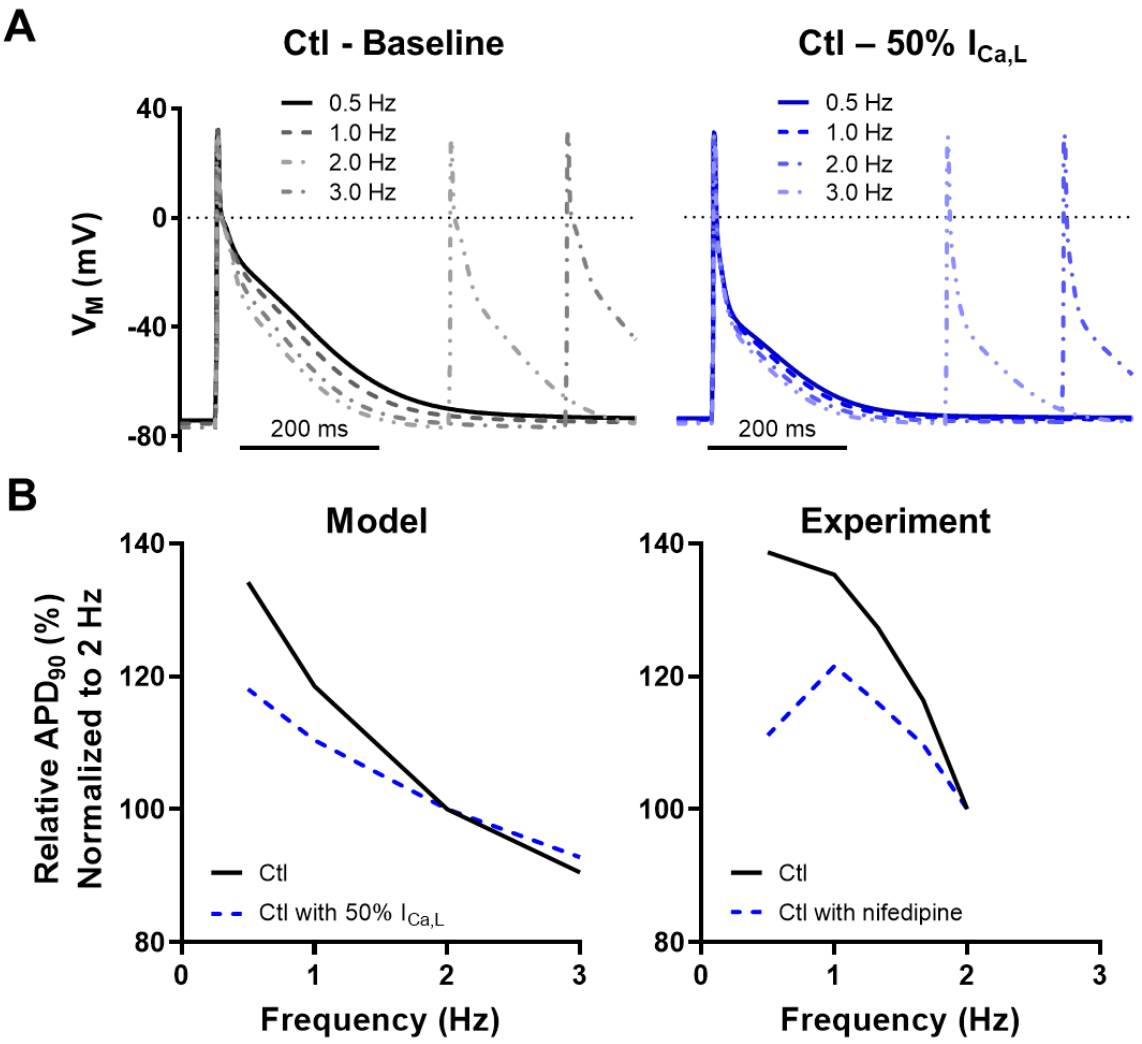

Figure S9. Response to L-type Ca^{2+} channel block. A, Time course of membrane potential in the Ctl model under baseline control conditions (**left**) and with 50% reduction in the conductance of the L-type Ca^{2+} current ($I_{Ca,L}$; **right**). **B,** Frequency dependence of action potential duration (APD_{90}; normalized to the value at 2-Hz pacing) assessed with normal (solid black line) or reduced (dashed blue line) $I_{Ca,L}$ in simulations (**left**) and experiments[68] (**right**).

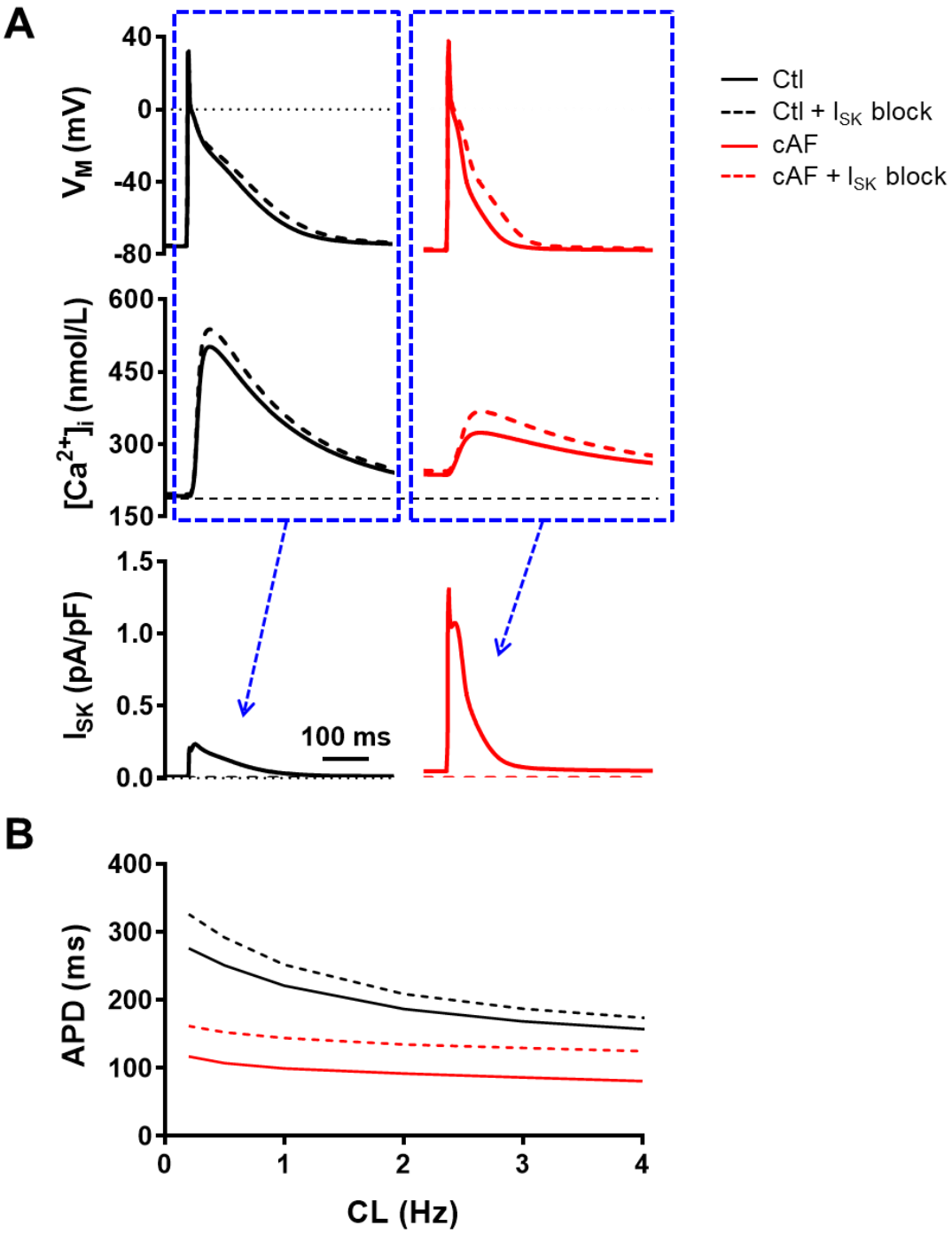

Figure S10. Effects of small-conductance Ca^{2+}-activated K^+-current (I_{SK}) inhibition during regular pacing in Ctl and cAF. A, Simulated action potentials (APs), Ca^{2+}-transients and resulting small-conductance I_{SK} in the Ctl (left) and cAF (right) versions of the novel human atrial cardiomyocyte model. Dashed lines represent AP and Ca^{2+}-transient during complete I_{SK}-block. **B,** Rate-dependence of AP duration (APD) in Ctl (black lines) and cAF (red lines) model versions in the absence (solid lines) or presence (dashed lines) of I_{SK}-inhibition.

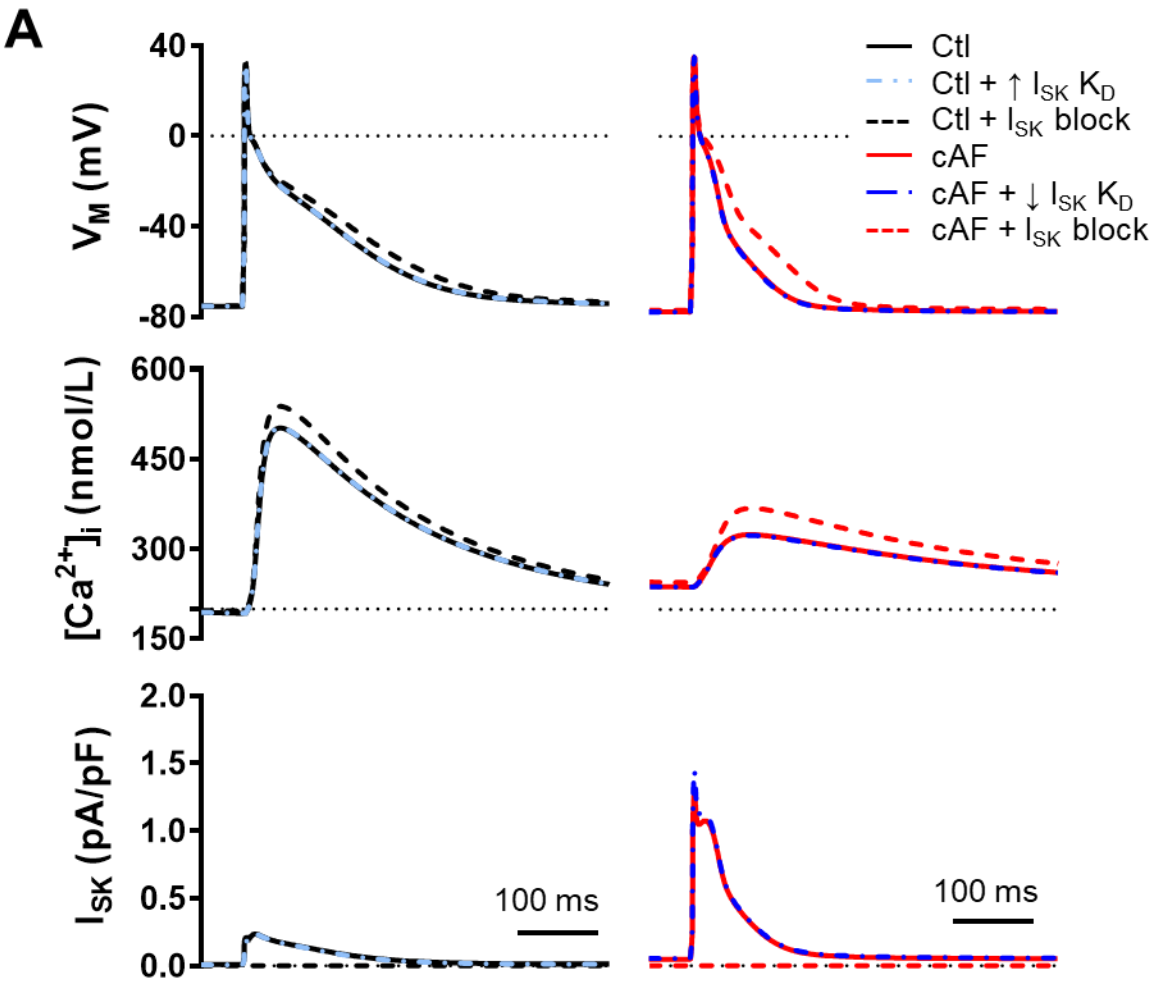

Figure S11. Impact of changes in the Ca^{2+} affinity (K_D) of small-conductance Ca^{2+}-activated K^+ channels on I_{SK} and action potential (AP) repolarization. A, APs (**top**), Ca^{2+} transients (**middle**) and I_{SK} (**bottom**) at 1 Hz pacing for the default Ctl (**left**) and cAF (**right**) model configurations (solid lines), in the presence of complete I_{SK} block (dashed lines) or in models with a lower affinity (larger K_D, ~330 nmol/L) in Ctl and higher affinity (lower K_D, ~230 nmol/L) in cAF to obtain the experimentally observed 100-nmol/L difference between Ctl and cAF cardiomyocytes (dash-dotted blue lines).

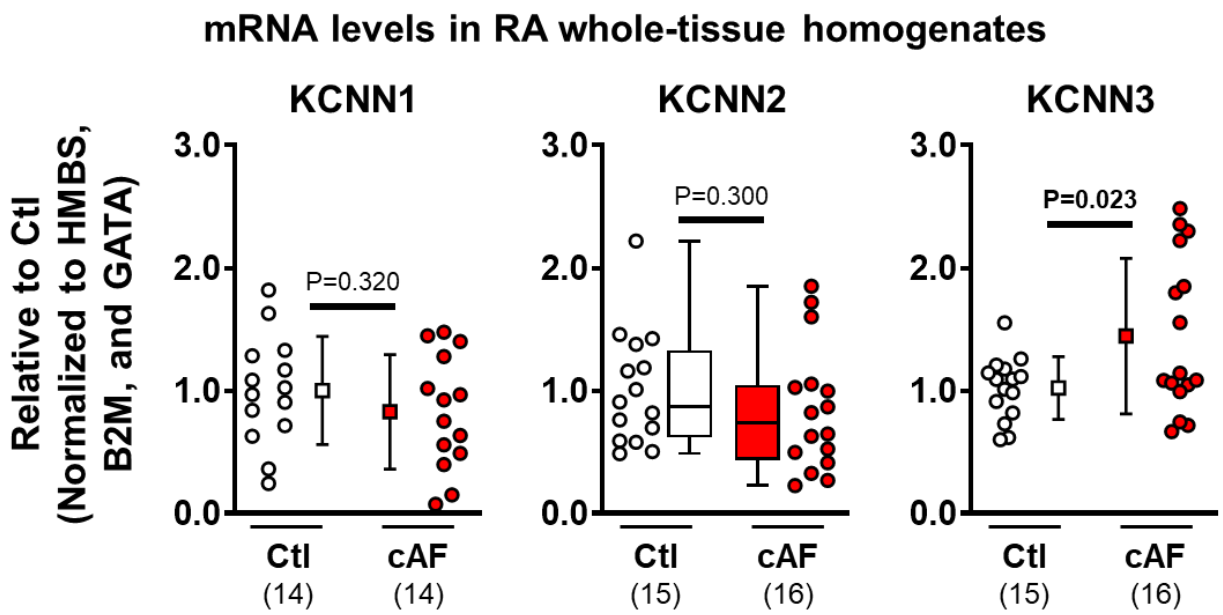

Figure S12. mRNA levels of small-conductance Ca^{2+}-activated K^+ (SK)-channel isoforms. mRNA levels of KCNN1, KCNN2 and KCNN3 (encoding for SK1, SK2 and SK3, respectively) in human right atrial (RA) whole-tissue homogenates of Ctl- and cAF-patients. N-numbers indicate number of patients. *P<0.05 vs. Ctl based on unpaired Student's *t*-test (KCNN1, KCNN3) or Mann-Whitney test (KCNN2).

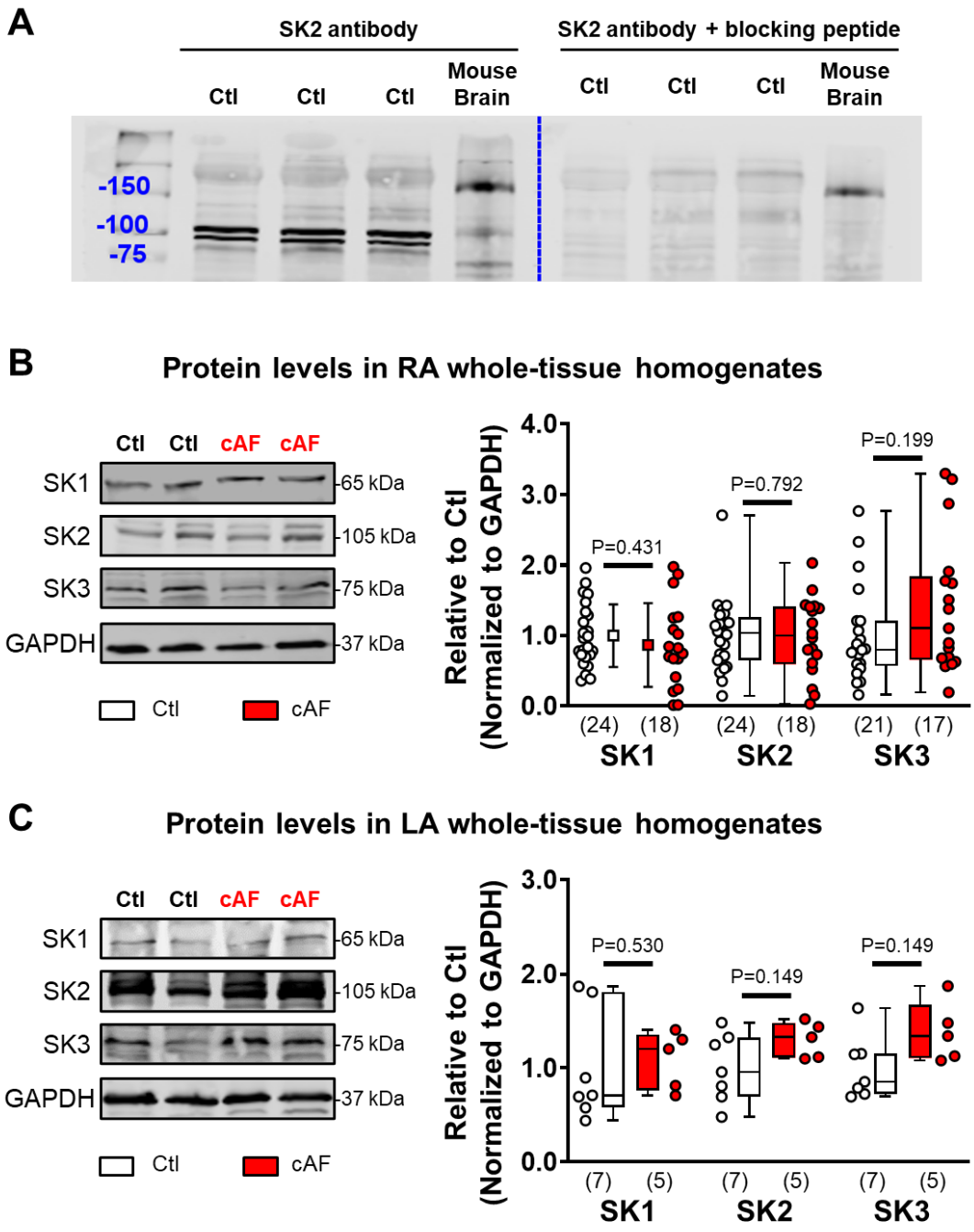

Figure S13. Protein levels of small-conductance Ca^{2+}-activated K^+ (SK)-channel isoforms (SK1-3). A, Validation of the 105 kDa band observed with the SK2 antibody in human right-atrial (RA) whole-tissue homogenates using a blocking peptide. Mouse brain tissue was used as a positive control. **B,** Representative Western blots (**left**) and quantification of SK1, SK2 and SK3 proteins in RA whole-tissue homogenates from Ctl- and cAF-patients. **C,** Similar to panel **B** for left-atrial (LA) whole-tissue homogenates. N-numbers indicate number of patients. *P<0.05 vs. Ctl based on unpaired Student's *t*-test (RA SK1) or Mann-Whitney test (all other comparisons).

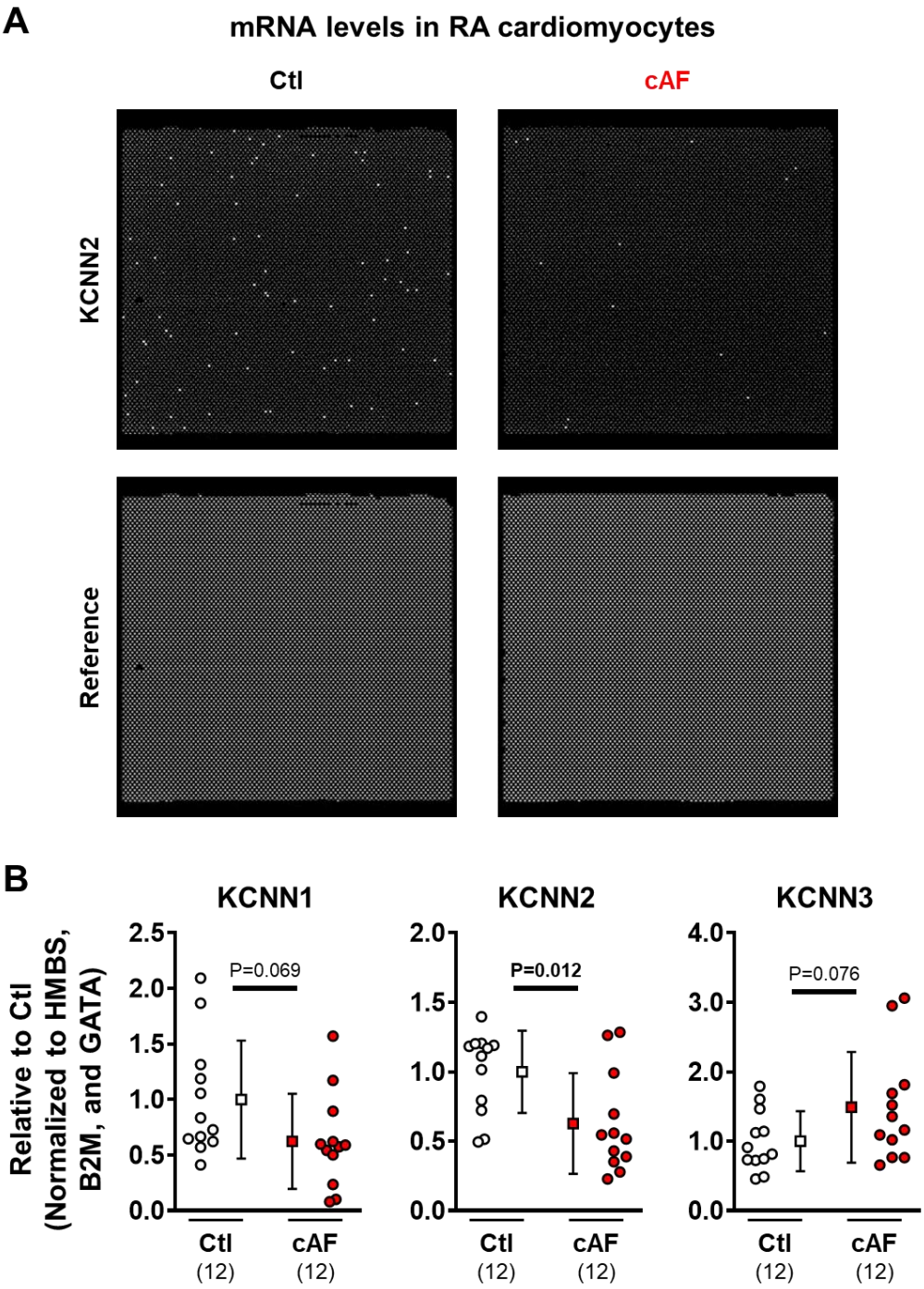

Figure S14. mRNA levels of small-conductance Ca^{2+}-activated K^+ (SK)-channel isoforms in right-atrial (RA) cardiomyocytes. A, Representative digital PCR images and corresponding reference images of KCNN2 in RA-cardiomyocytes from Ctl- and cAF-patients. Each well contains 8500 partitions and copies/µL values are calculated based on the number of illuminated points and the reference channel. Representative examples of all SK-isoforms and housekeeping genes are shown in **Figure S15**. **B,** mRNA levels of KCNN1, KCNN2 and KCNN3 in RA-cardiomyocytes of Ctl- and cAF-patients. N-numbers indicate number of patients. P-values are based on unpaired Student's *t*-test.

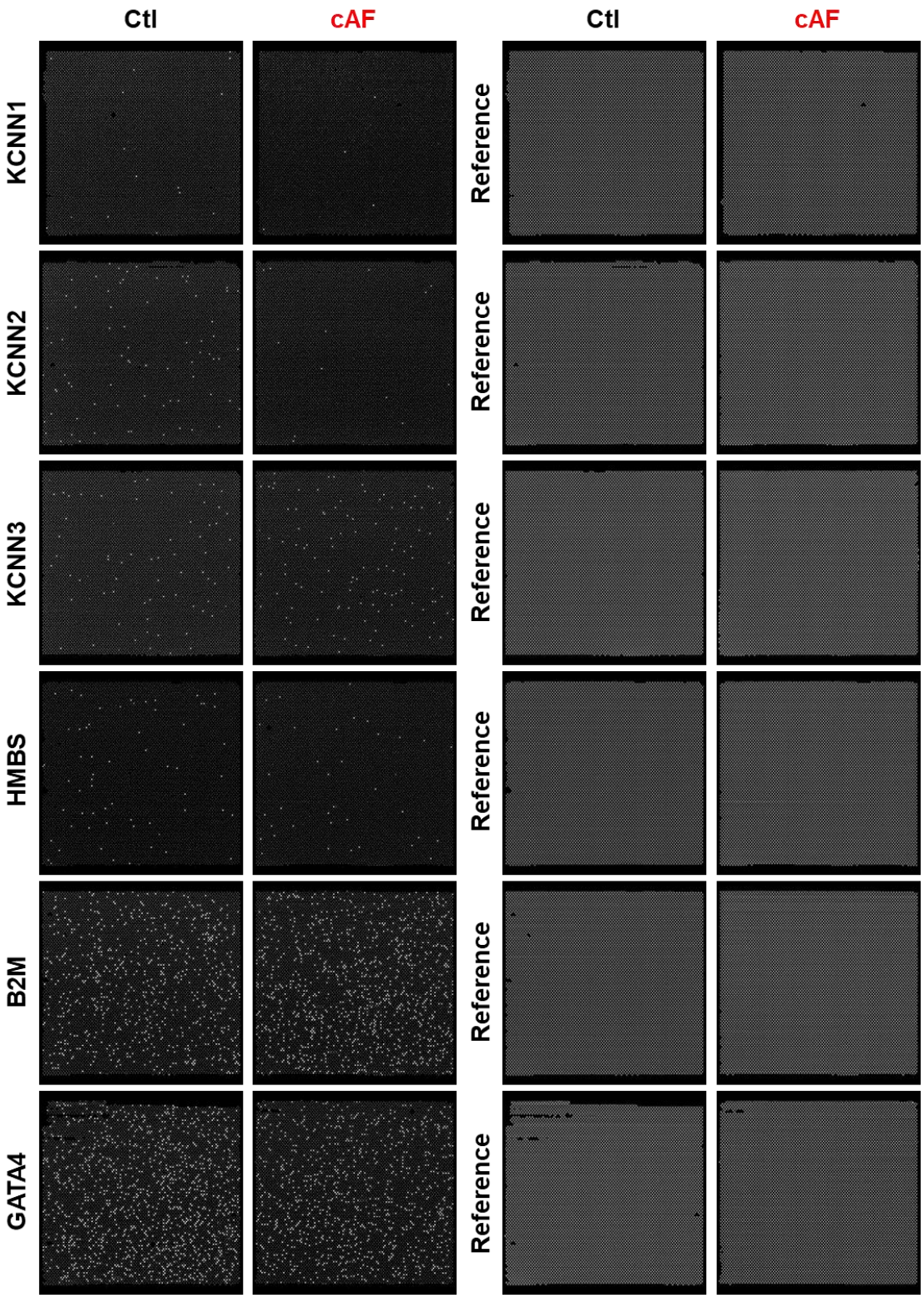

Figure S15. Representative digital PCR images and corresponding reference images of KCNN1, KCNN2, KCNN3 and the housekeeping genes HMBS, B2M and GATA4 in right-atrial cardiomyocytes from Ctl- and cAF-patients.

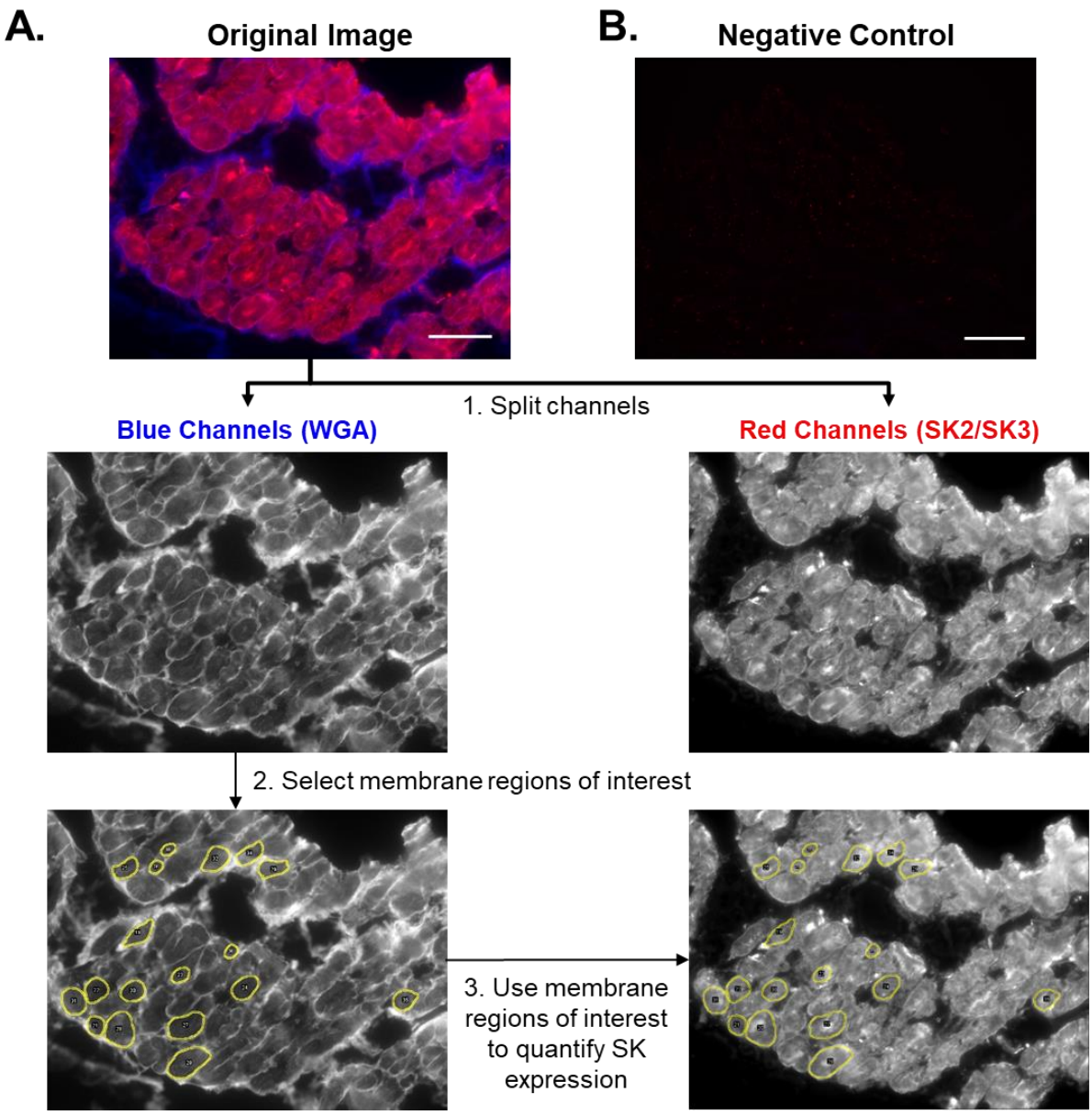

Figure S16. Methodology for immunostaining of small-conductance Ca^{2+}-activated K^+ (SK) channels in human right- or left-atrial tissue slices. A, Images were obtained from tissue slices stained with antibodies against wheat germ agglutinin (WGA) and SK2 or SK3. The channels were split and the WGA signal was used to identify cardiomyocytes with clear membrane staining. In these cardiomyocytes the membrane was traced and these regions of interest were subsequently used to determine the relative membrane to cytosol fluorescence intensity ratio of SK2 and SK3. Scale bar represents 50 µm. **B,** Negative control stained without primary antibodies. Scale bar represents 200 µm.

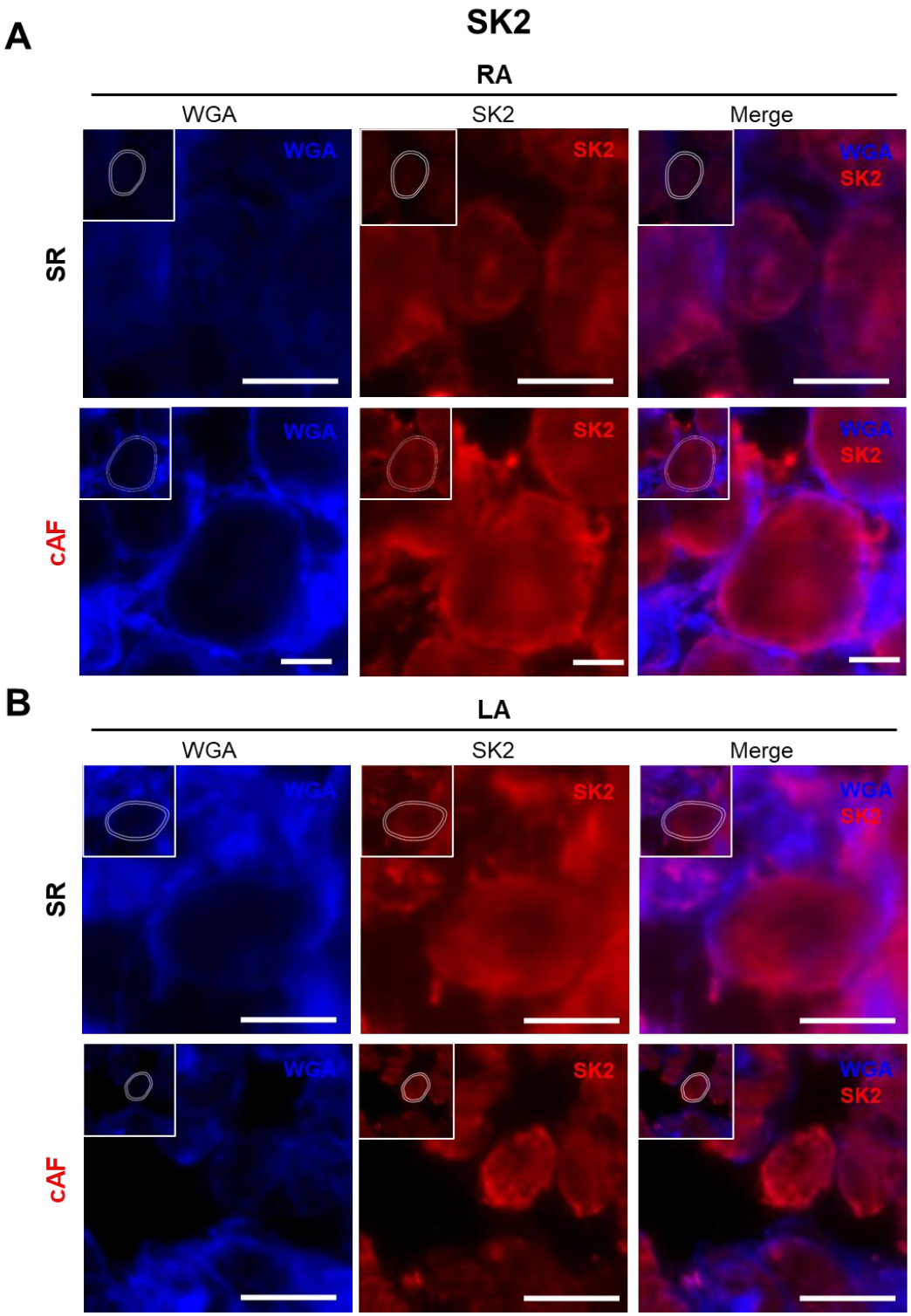

Figure S17. Representative examples of wheat germ agglutinin (WGA) and small-conductance Ca^{2+}-activated K^+ channel 2 (SK2) immunostaining. A,B, WGA staining (blue), SK2 staining (red) and their combination in right-atrial (RA; panel **A**) and left-atrial (LA; panel **B**) tissue slices from Ctl- and cAF-patients. Insets show membrane regions defined based on WGA staining. Scale bars represent 10 μm.

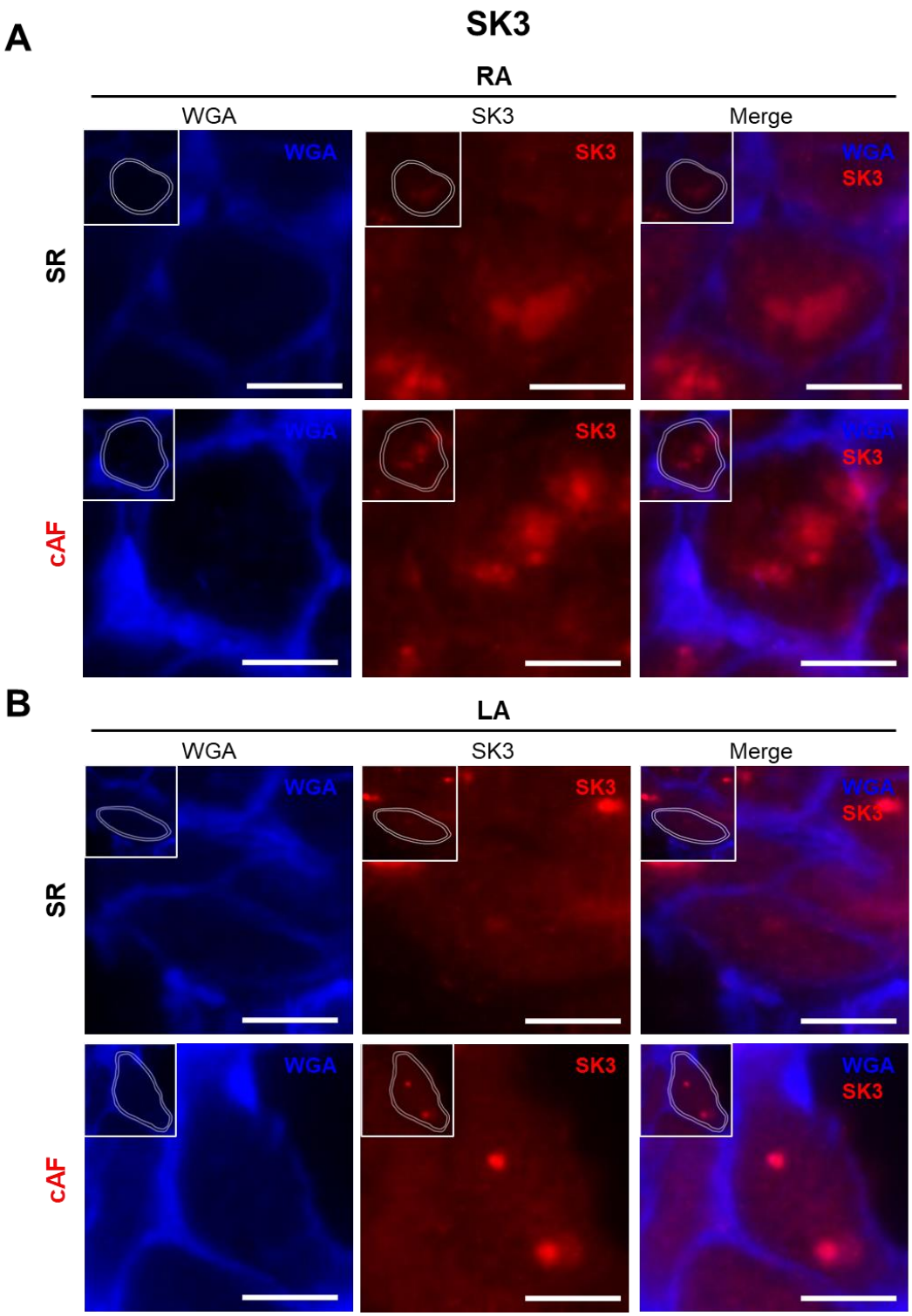

Figure S18. Representative examples of wheat germ agglutinin (WGA) and small-conductance Ca^{2+}-activated K^+ channel 3 (SK3) immunostaining. A,B, WGA staining (blue), SK3 staining (red) and their combination in right-atrial (RA; panel **A**) and left-atrial (LA; panel **B**) tissue slices from Ctl- and cAF-patients. Insets show membrane regions defined based on WGA staining. Scale bars represent 10 μm.

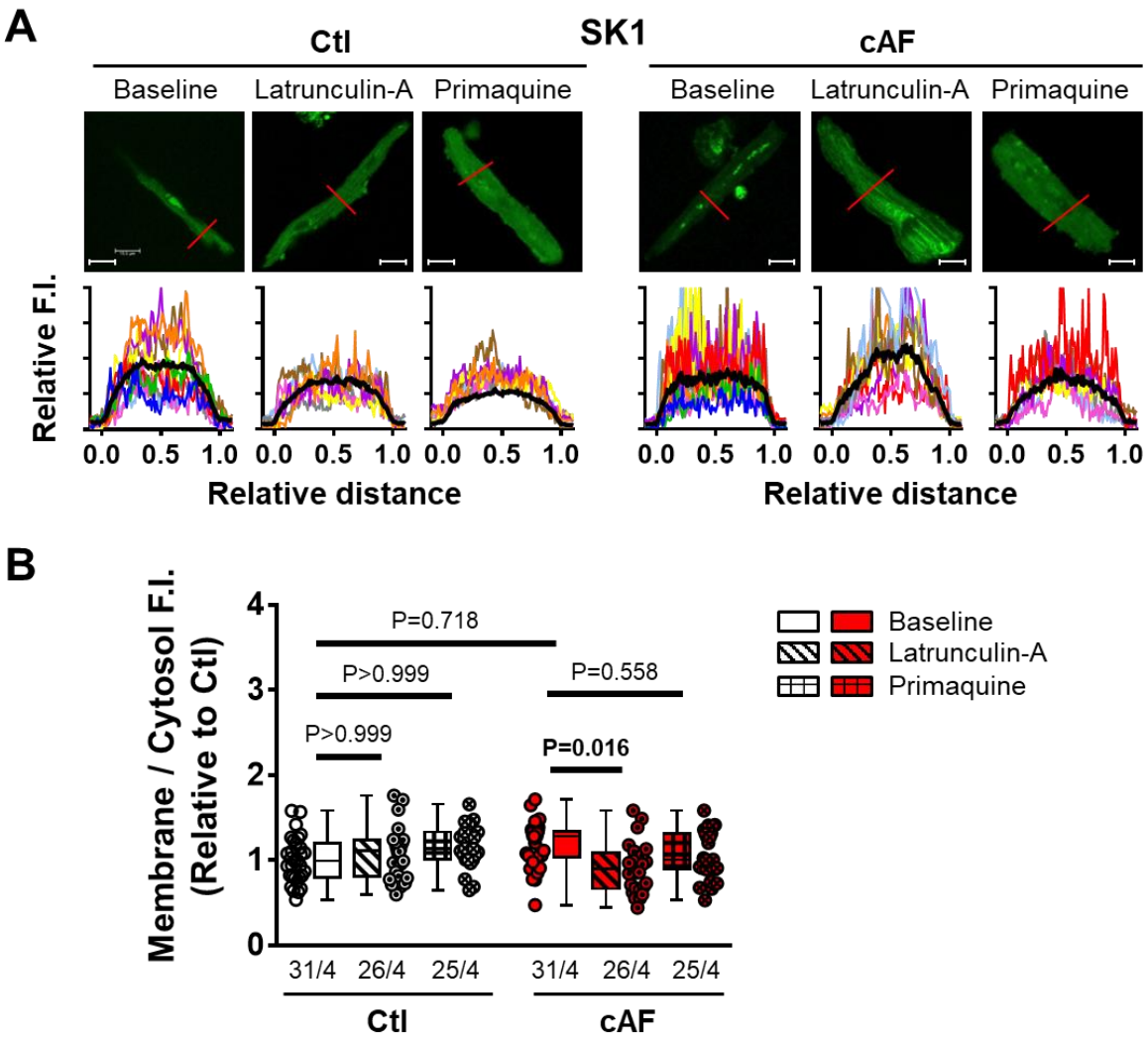

Figure S19. Membrane localization and trafficking of small-conductance Ca^{2+}-activated K^{+}-channel 1 (SK1). A, Representative immunocytochemistry of SK1 in right-atrial (RA)-cardiomyocytes from Ctl- and cAF-patients at baseline or after inhibition of anterograde or retrograde protein trafficking with latrunculin-A (1-µmol/L for 2-hours) or primaquine (120-µmol/L for 4-hours), respectively. Lower panels show transversal line profiles of fluorescence intensity (F.I.) for all cardiomyocytes (thin colored lines), as well as the average across all cells (thick black lines). Scale bars indicate 15-µm. **B,** Average F.I. of SK1 at the membrane (first and last 10% of cell width) compared to the cytosol (middle 80%) for Ctl and cAF with or without latrunculin-A (diagonal-patterned bars) or primaquine (hashed bars). Data are normalized to RA-cardiomyocytes from Ctl-patients at baseline. N-numbers indicate numbers of cardiomyocytes/patients. P-values are based on multilevel mixed models with log-transformed data to account for non-independent measurements in multiple cells from individual patients and are Bonferroni-corrected to account for multiple comparisons.

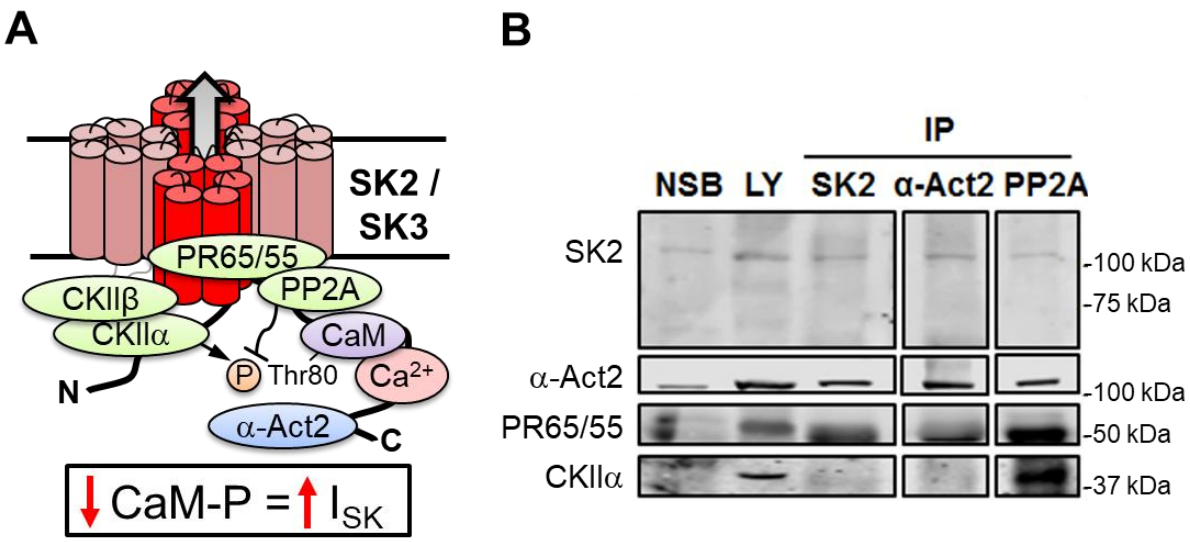

Figure S20. The small-conductance Ca^{2+}-activated K^+ (SK) channel macromolecular complex. A, Schematic representation of the SK-channel macromolecular complex, including phosphorylation-dependent regulation of calmodulin (CaM). **B,** Representative Western blots of SK2, α-actinin2 (α-Act2), the protein phosphatase 2A (PP2A)-regulatory subunit PR65/55 and casein kinase IIα (CKIIα) in right-atrial lysates (Ly) or immunoprecipitates (IP) of SK2, α-Act2 or PP2A, confirming their presence as part of the SK2 macromolecular complex. NSB refers to a negative control for non-specific binding (beads and lysates without antibody).

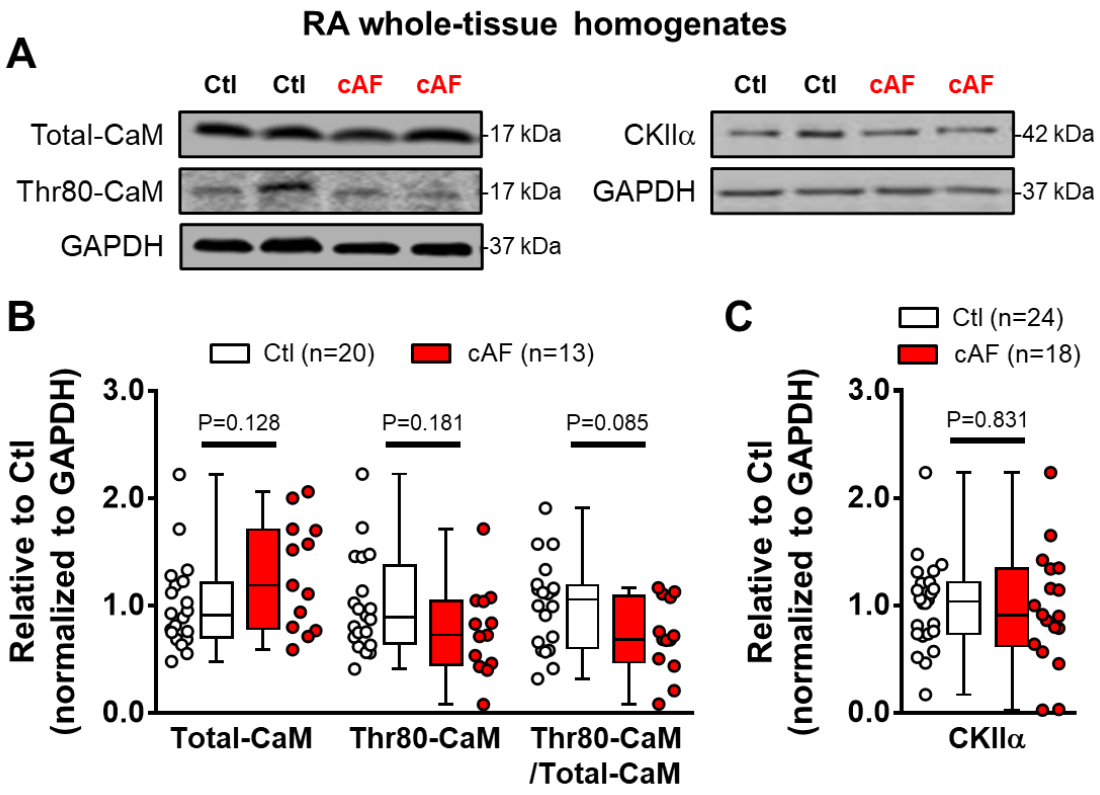

Figure S21. cAF-associated remodeling of calmodulin (CaM) and casein kinase IIα (CKIIα) in right-atrial (RA) whole-tissue homogenates. A, Representative Western blots of total and Thr80-phosphorylated CaM (**left**) and CKIIα (**right**) in RA whole-tissue homogenates of Ctl- and cAF-patients. GAPDH was used as loading control. **B,** Quantification of total and Thr80-phosphorylated calmodulin, as well as relative phosphorylation ratio in Ctl- and cAF-patients. **C,** Quantification of protein levels of CKIIα in RA whole-tissue homogenates of Ctl and cAF patients. N-numbers indicate number of patients. P-values are based on Mann-Whitney test.

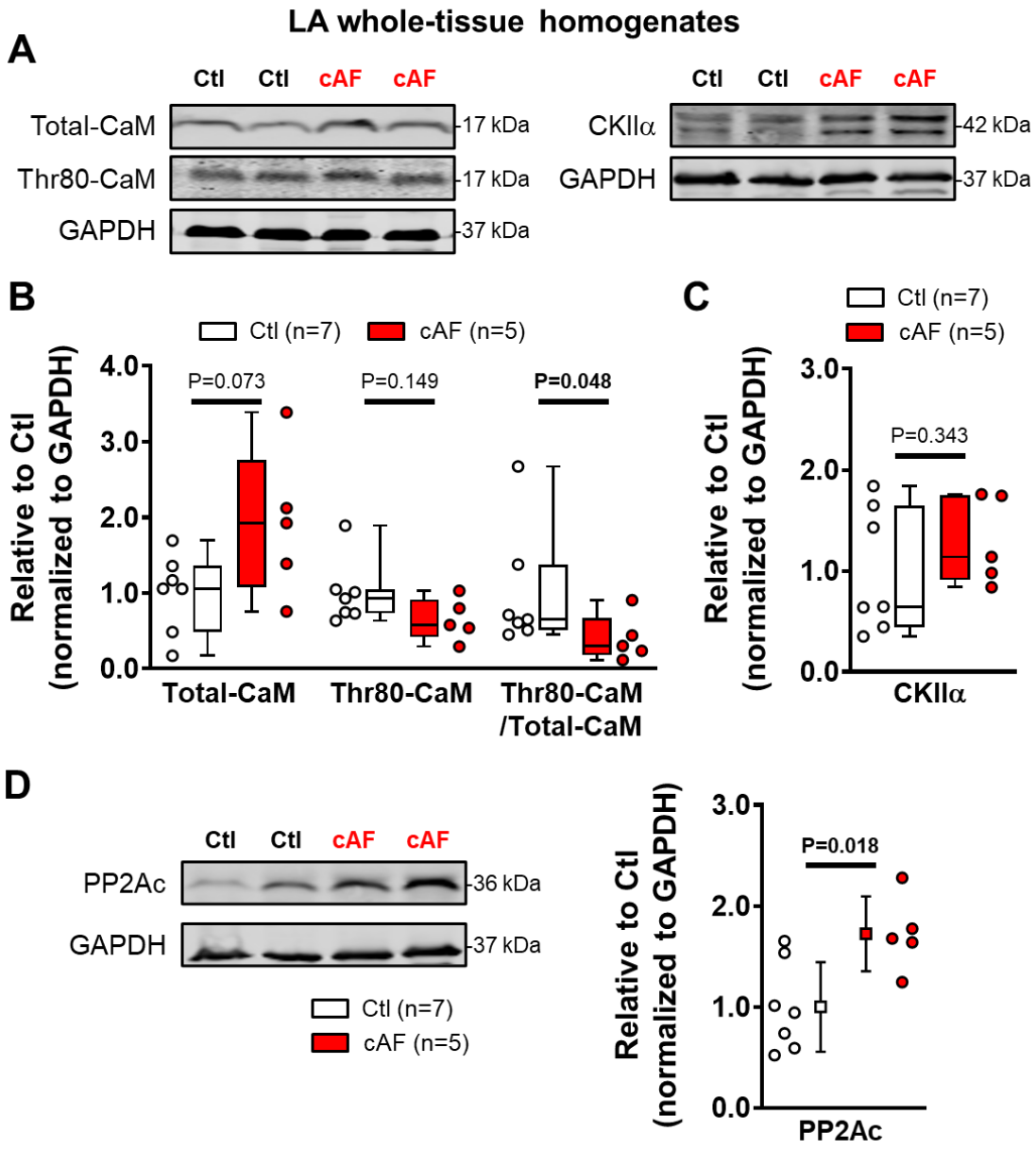

Figure S22. cAF-associated remodeling of calmodulin, casein kinase IIα (CKIIα), and catalytic protein phosphatase type-2a (PP2Ac) in left-atrial (LA) whole-tissue homogenates. A, Representative Western blots of total and Thr80-phosphorylated CaM (**left**) and CKIIα (**right**) in LA whole-tissue homogenates of Ctl- and cAF-patients. GAPDH was used as loading control. **B,** Quantification of total and Thr80-phosphorylated calmodulin, as well as relative phosphorylation ratio in Ctl- and cAF-patients. **C,** Quantification of protein levels of CKIIα in LA whole-tissue homogenates of Ctl- and cAF-patients. **D,** Representative Western blots (**left**) and quantification (**right**) of PP2Ac protein levels in LA whole-tissue homogenates of Ctl- and cAF-patients. GAPDH was used as loading control. N-numbers indicate number of patients. P-values are based on Mann-Whitney test (**B,C**) or unpaired Student's *t*-test (**D**).

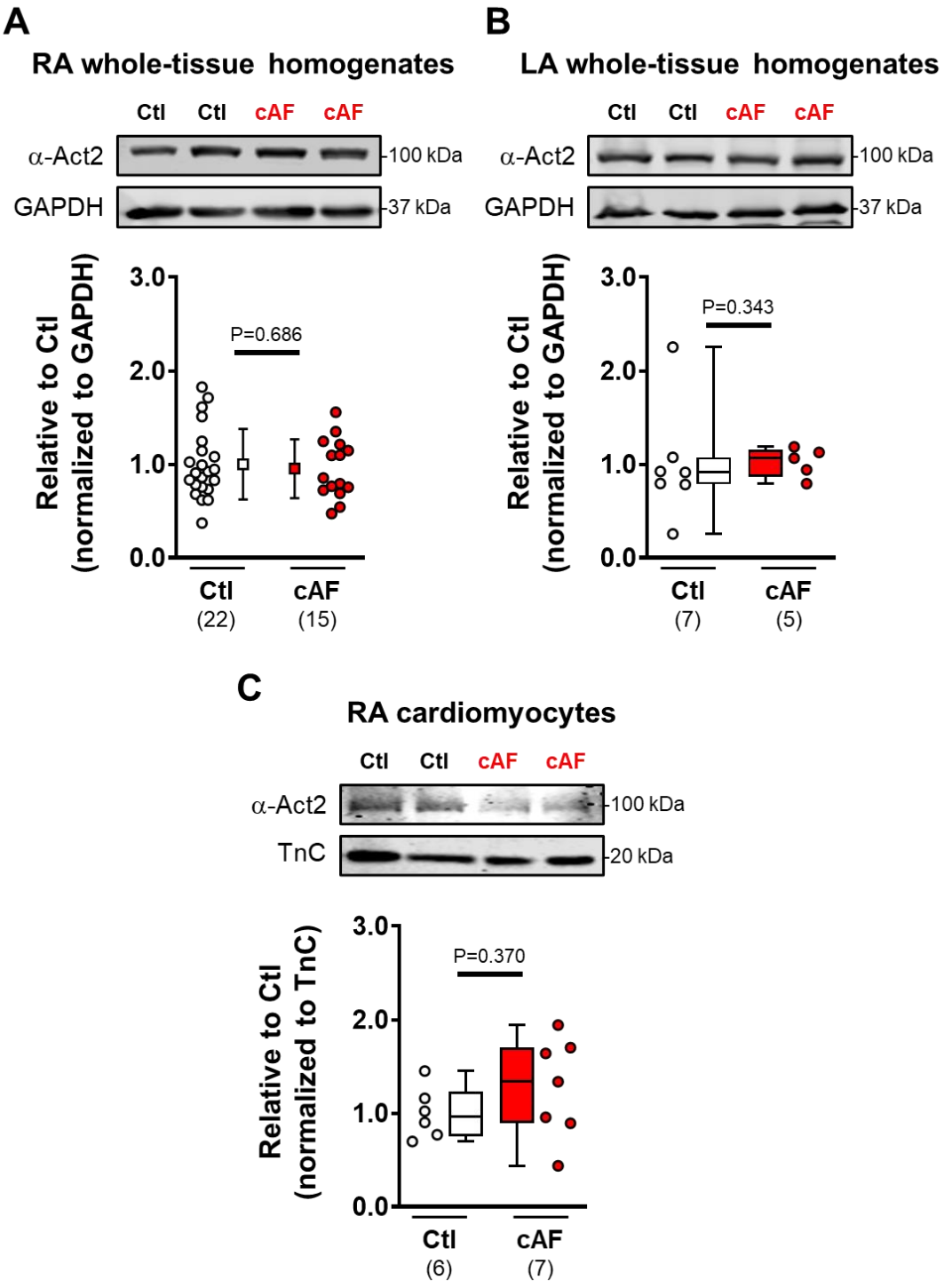

Figure S23. Protein levels of α-actinin2 (α-Act2) in Ctl- and cAF-patients. A-C, Representative Western blots (**top**) and quantification (**bottom**) of α-Act2 in right-atrial (RA) whole-tissue homogenates (**A**), left-atrial (LA) whole-tissue homogenates (**B**), or RA-cardiomyocytes (**C**) of Ctl- and cAF-patients. GAPDH and troponin-C (TnC) were used as loading controls. N-numbers indicate number of patients. P-values are based on Student's *t*-test (**A**) or Mann-Whitney test (**B,C**).

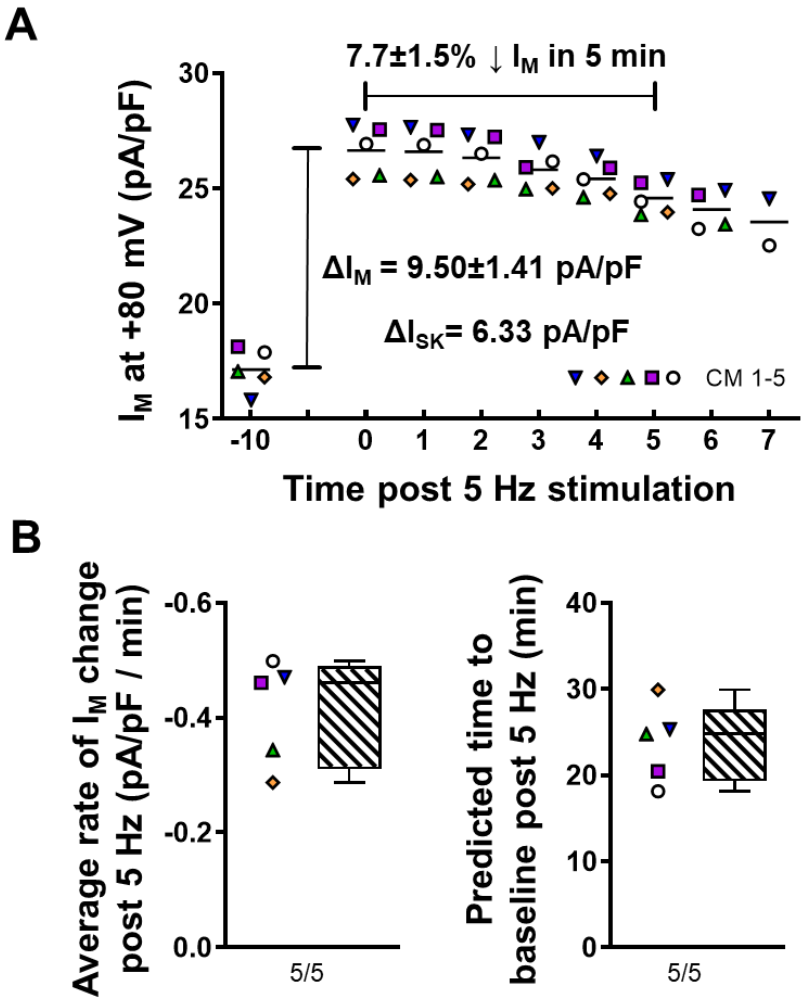

Figure S24. Reversibility of tachypacing-induced remodeling of membrane currents. A, Time course of total membrane current (I_M) in human right-atrial cardiomyocytes from Ctl patients at +80 mV before 10 minutes of 5 Hz stimulation and every minute after 5 Hz stimulation. The increase in total I_M due to 10 minutes of 5 Hz stimulation is indicated and compared to the increase in apamin-sensitive small-conductance Ca^{2+}-activated K^+ current (I_{SK}) identified in a separate subgroup of cells (data from **Figure 7B**). **B,** The average rate of IM decay after 10 minutes of 5 Hz stimulation (**left**) and the extrapolated time required to reach baseline I_M level based on rate of change and magnitude of tachypacing-induced I_M increase (**right**) in human right-atrial cardiomyocytes from Ctl patients. N-numbers indicate number of cardiomyocytes/patients.

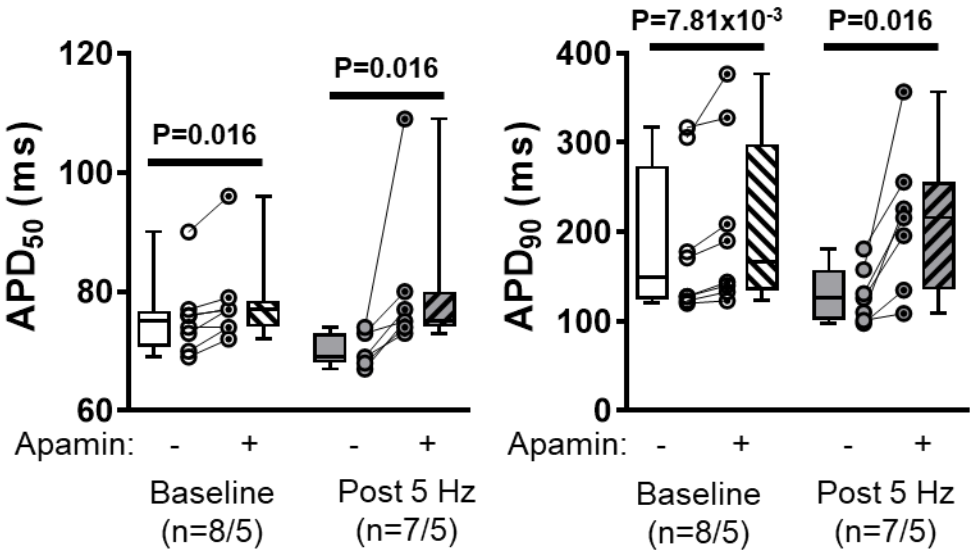

Figure S25. Effect of apamin on action potential duration (APD) parameters in right-atrial cardiomyocytes from Ctl-patients at baseline or after 10-minutes stimulation at 5 Hz. A, APD at 50% of repolarization (APD_{50}). **B,** APD at 90% of repolarization (APD_{90}). N-numbers indicate numbers of cardiomyocytes/patients. P-values are based on Wilcoxon signed rank test for paired samples.

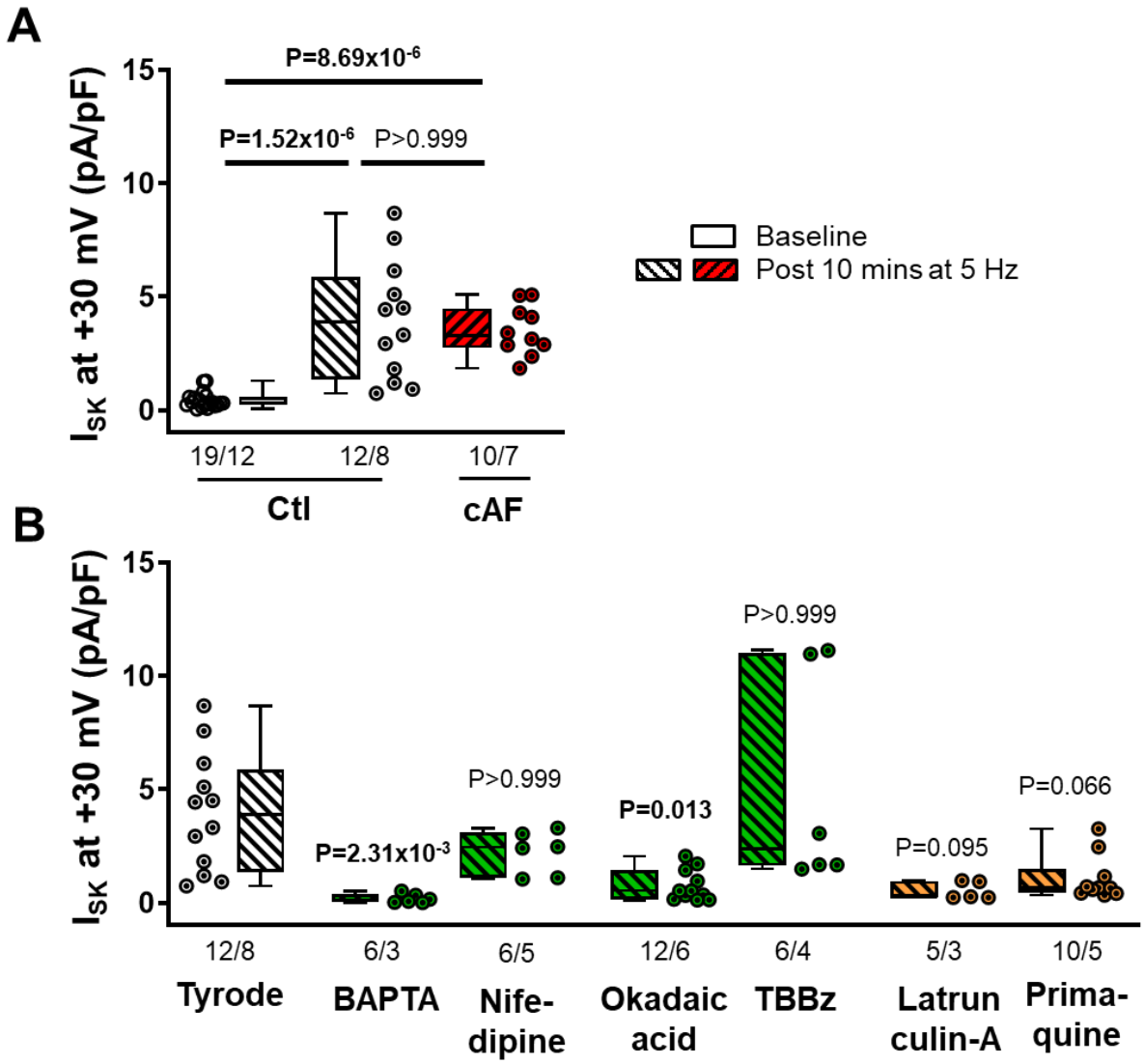

Figure S26. Tachycardia-dependent upregulation of small-conductance Ca^{2+}-activated K^+ (SK)-channels. A, Apamin (100-nmol/L)-sensitive I_{SK} at +30 mV in right-atrial Ctl-cardiomyocytes at baseline (open symbols) and from RA-cardiomyocytes from Ctl- or cAF-patients after 10-minutes of 5-Hz activation (diagonal-patterned bars). **B,** Apamin-sensitive I_{SK} at +30 mV in RA-cardiomyocytes from Ctl-patients after 10-minutes of 5-Hz activation after pre-incubation with the Ca^{2+}-chelator BAPTA-AM (30-µmol/L for 1-hour), L-type Ca^{2+}-channel blocker nifedipine (1-µmol/L for 3-mins), PP2A-inhibitor okadaic acid (10-nmol/L for 1-hour) or casein kinase type-II inhibitor TBBz (10-µmol/L for 1-hour) (green bars; all affecting SK-channel gating), or latrunculin-A (1-µmol/L for 2-hours) and primaquine (120-µmol/L for 4-hours) (orange bars; both affecting SK-channel trafficking). N-numbers indicate numbers of cardiomyocytes/patients. P-values are based on multilevel mixed models with log-transformed data to account for non-independent measurements in multiple cells from individual patients and are Bonferroni-corrected to account for multiple comparisons. Results correspond to the data shown at +80 mV in **Figure 7**.

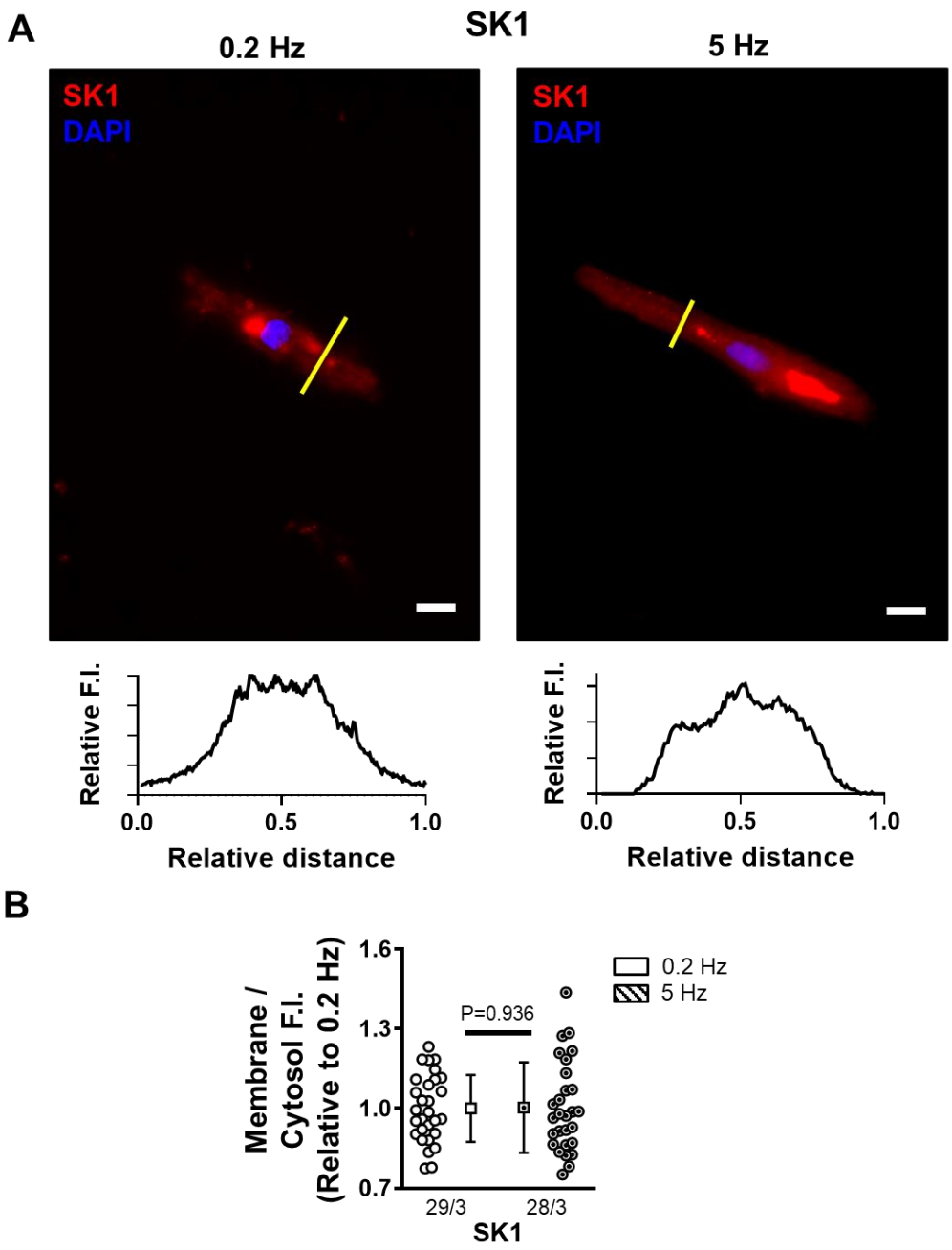

Figure S27. Membrane localization of small-conductance Ca^{2+}-activated K^+ (SK)-1 channels after field stimulation. A, Representative immunocytochemistry of SK1 in right-atrial cardiomyocytes from Ctl-patients after 10 minutes of field stimulation at 0.2 Hz or 5 Hz. Lower panels show transversal line profiles of fluorescence intensity (F.I.). Scale bars indicate 10-µm. **B,** Average F.I. of SK1 at the membrane (first and last 10% of cell width) compared to the cytosol (middle 80%) after 10 minutes of field stimulation at 0.2 Hz or 5 Hz. Data are normalized to 0.2 Hz. N-numbers indicate numbers of cardiomyocytes/patients. P-values are based on multilevel mixed models to account for non-independent measurements in multiple cells from individual patients and take into account that cardiomyocytes from the same patients were used for 0.2 Hz and 5 Hz.

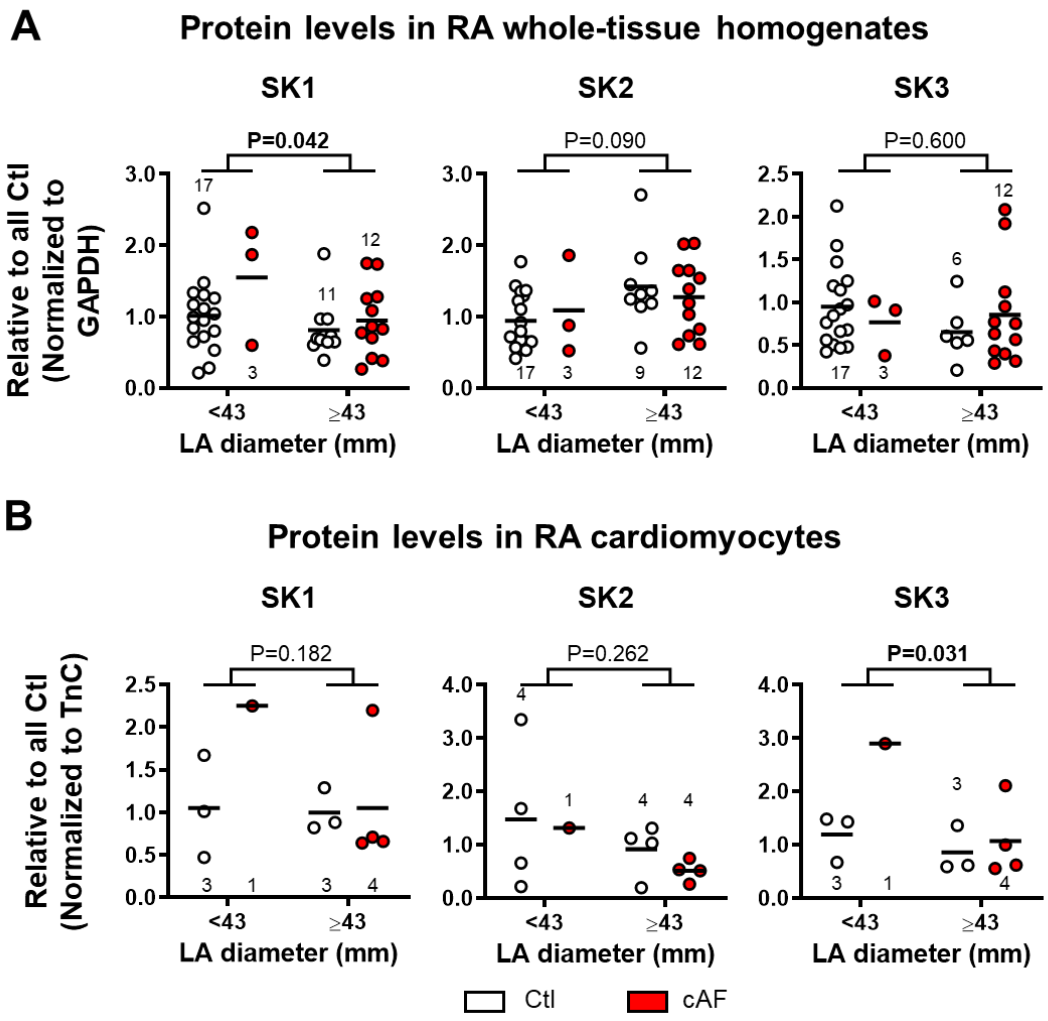

Figure S28. Association between-atrial (LA) diameter and right-atrial (RA) SK-channel subunit protein levels. A-B, two-way ANOVA analyses of rhythm and LA diameter for SK1-3 in RA whole-tissue homogenates (**A**, based on **Figure S13**), or RA-cardiomyocytes (**B,** based on **Figure 2C**). N-numbers indicate number of patients. P-values are for the factor LA diameter in the two-way ANOVA.

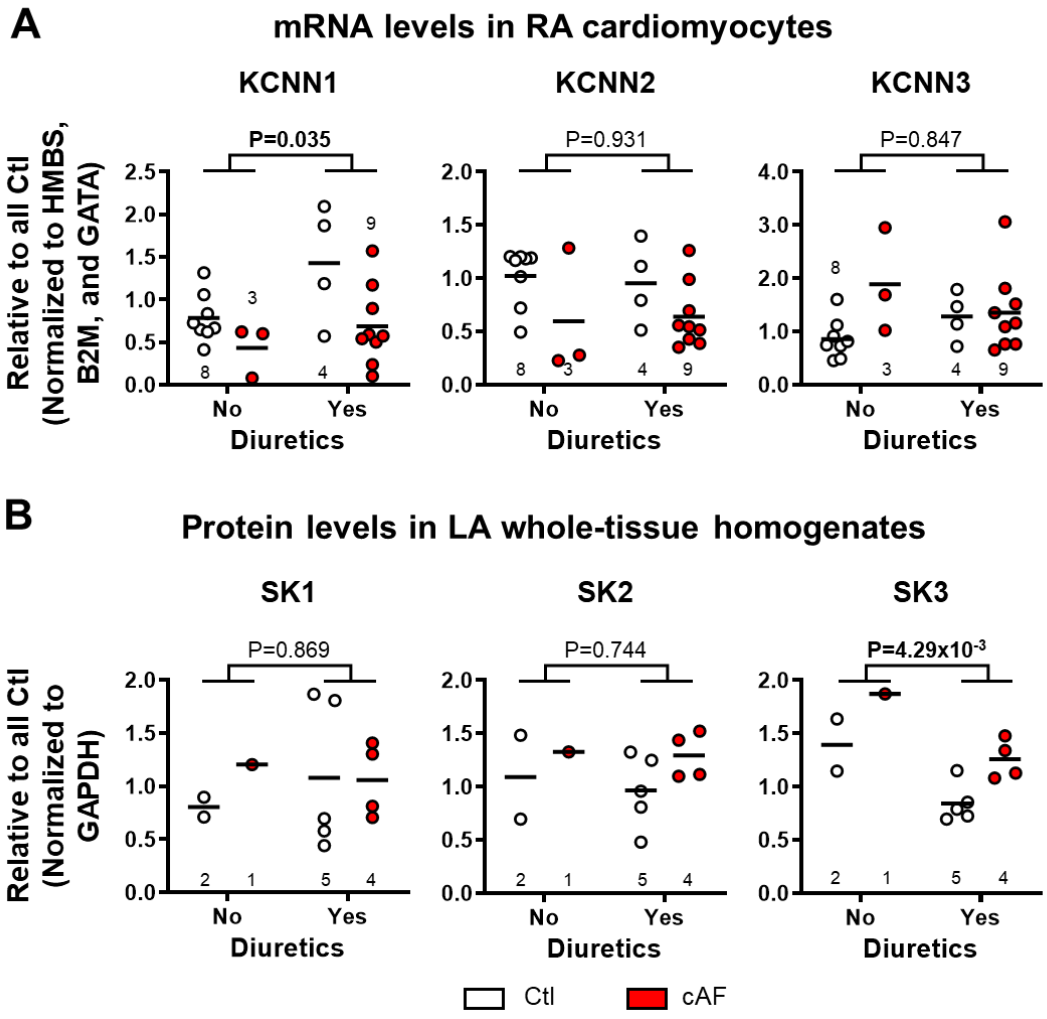

Figure S29. Association between diuretic use and SK-channel subunit levels. A, two-way ANOVA analyses of rhythm and diuretic use for *KCNN1-3* in right-atrial (RA) cardiomyocytes (based on **Figure S12**). **B,** two-way ANOVA analyses of rhythm and diuretic use for SK1-3 in left-atrial (LA) whole-tissue homogenates (based on **Figure S13**). N-numbers indicate number of patients. P-values are for the factor diuretics in the two-way ANOVA.

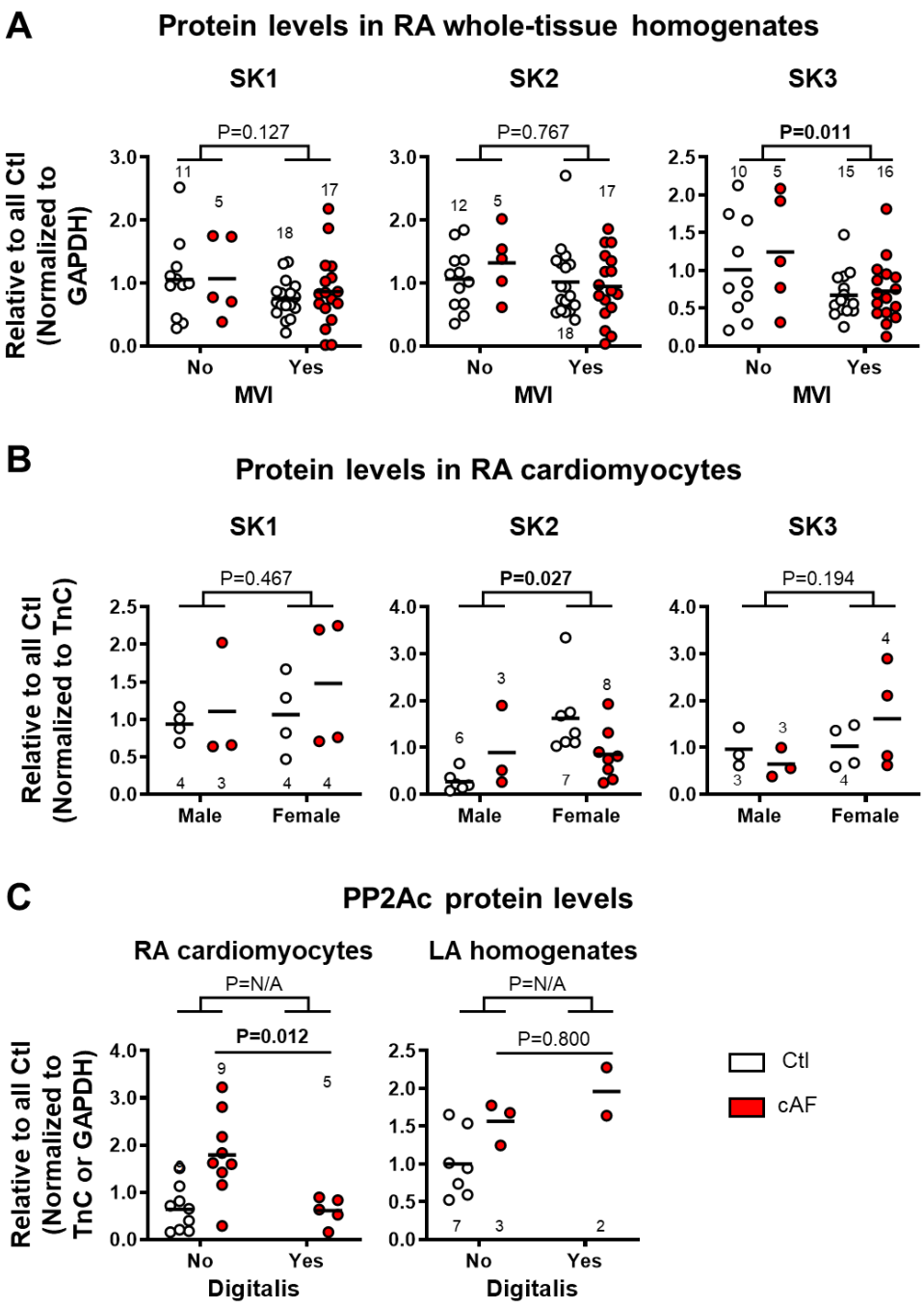

Figure S30. Significant associations between further clinical variables and SK-subunit or protein phosphatase 2Ac (PP2Ac) protein levels (see Table S13). A-B, two-way ANOVA analyses of rhythm and mitral valve insufficiency (MVI; **A**) or sex (**B**) for SK1-3 in right-atrial (RA) whole-tissue homogenates (**A**, based on **Figure S13**) or RA-cardiomyocytes (**B**, based on **Figure 2C**). **C,** two-way ANOVA analyses of rhythm and digitalis use for PP2Ac in RA-cardiomyocytes (based on **Figure 6D**) or left-atrial (LA) whole-tissue homogenates (based on **Figure S12**). N-numbers indicate number of patients. P-values are for the factors MVI, sex or digitalis in the two-way ANOVA. In addition, P-values for Mann-Whitney comparisons between cAF patients with or without digitalis are shown in panel **C**.

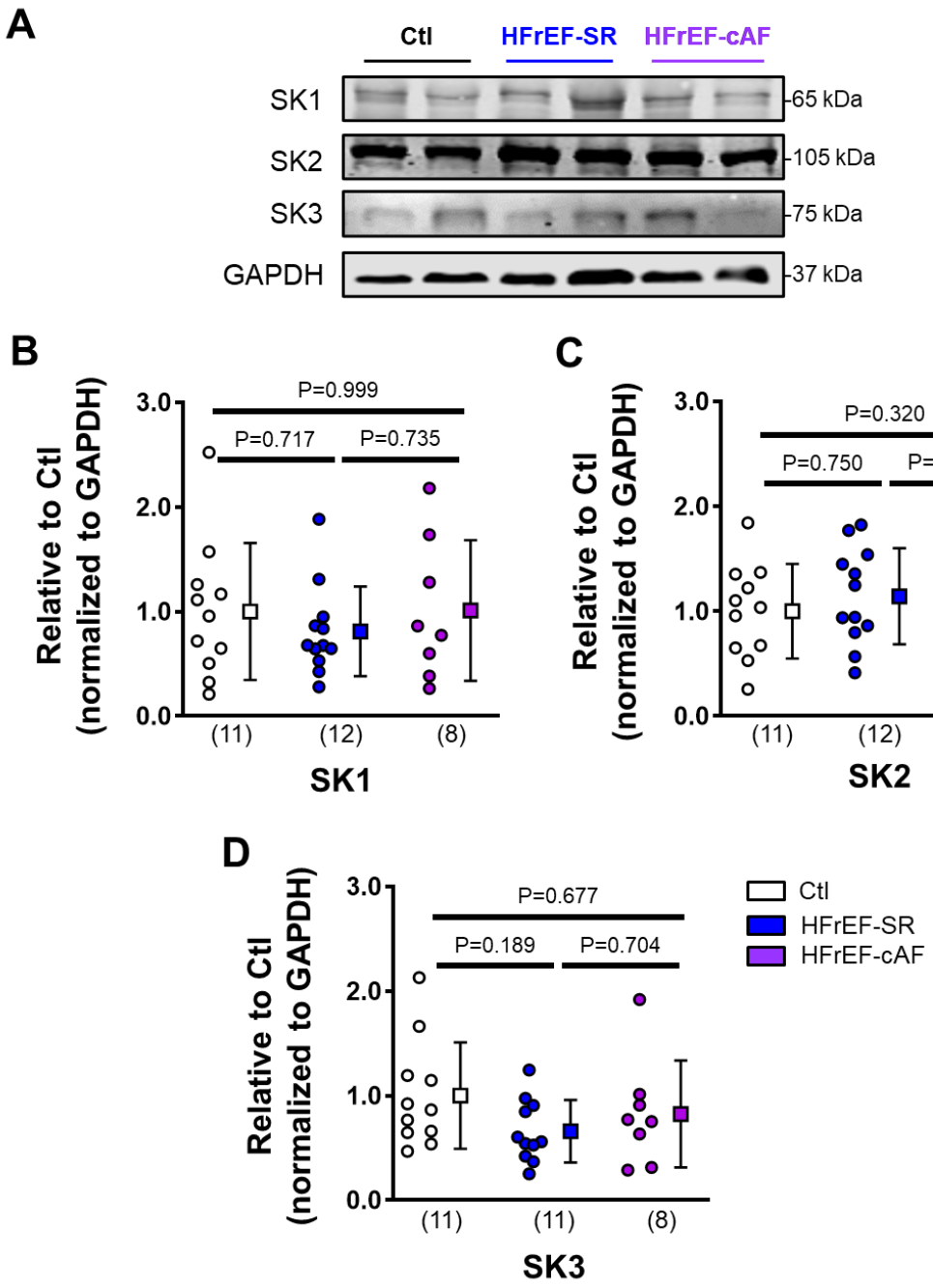

Figure S31. Effect of heart failure with reduced left-ventricular ejection fraction (HFrEF; LVEF ≤35%) on small-conductance Ca^{2+}-activated K^+ (SK) channel protein levels. A, Representative Western blots of SK1, SK2 and SK3 in right-atrial (RA) whole-tissue homogenates of Ctl-patients (no HFrEF, no history of AF), HFrEF-patients without AF (HFrEF-SR), and HFrEF-patients with cAF (HFrEF-cAF). GAPDH was used as loading control. **B-D,** Quantification of protein levels of SK1 (**B**), SK2 (**C**) and SK3 (**D**) in RA whole-tissue homogenates of Ctl, HFrEF-SR and HFrEF-cAF patients. N-numbers indicate number of patients. P-values are based on one-way ANOVA with Tukey's multiple comparisons test.

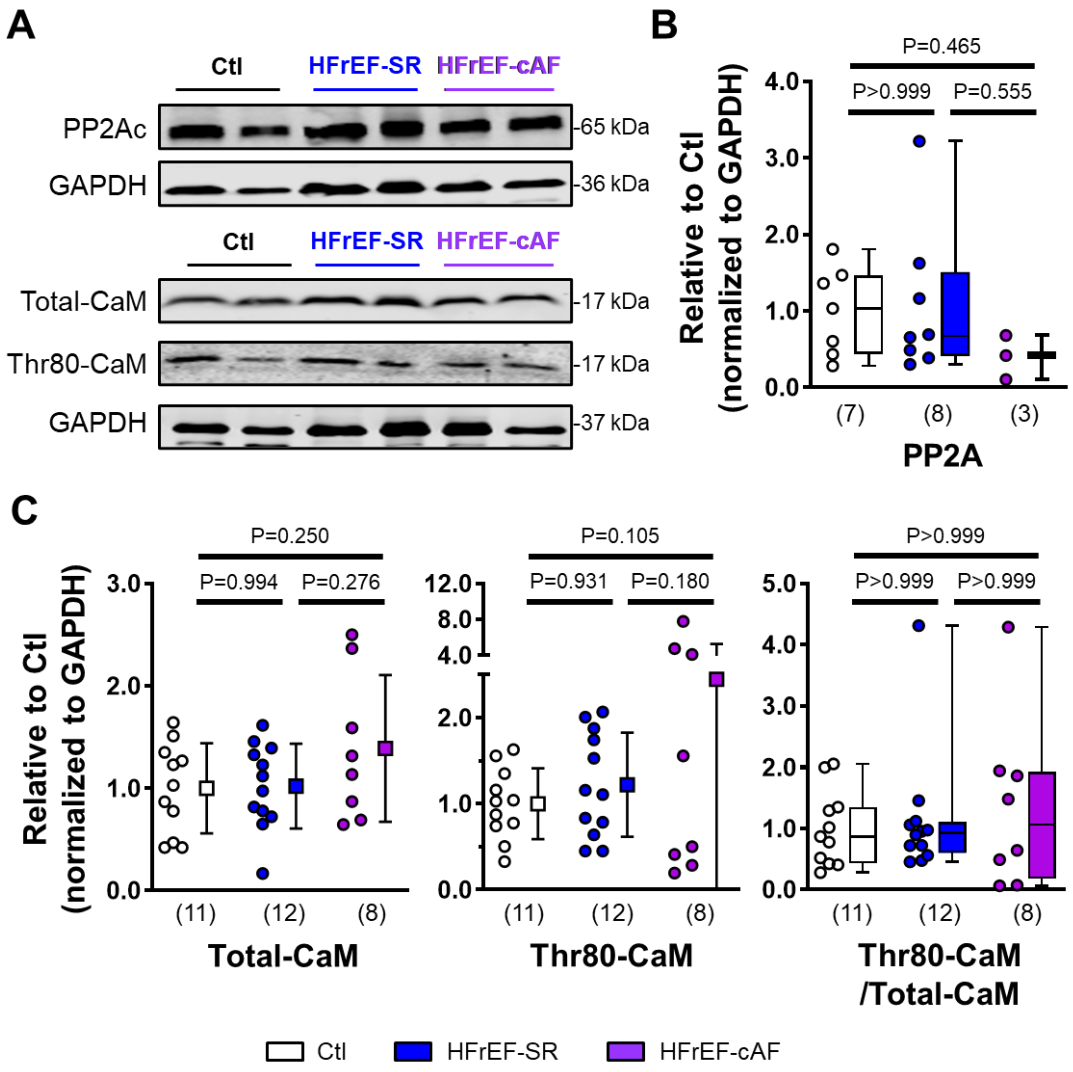

Figure S32. Effect of heart failure with reduced left-ventricular ejection fraction (HFrEF; LVEF ≤35%) on protein levels of calmodulin (CaM) and catalytic protein phosphatase type-2a (PP2Ac). A, Representative Western blots of PP2Ac, as well as total and Thr80-phosphorylated CaM in right-atrial (RA) whole-tissue homogenates of Ctl-patients (no HFrEF, no history of AF), HFrEF-patients without AF (HFrEF-SR), and HFrEF-patients with cAF (HFrEF-cAF). GAPDH was used as loading control. **B,** Quantification of PP2Ac protein levels in RA whole-tissue homogenates of Ctl, HFrEF-SR and HFrEF-cAF patients. **C,** Quantification of total and Thr80-phosphorylated calmodulin, as well as relative phosphorylation ratio in RA whole-tissue homogenates of Ctl, HFrEF-SR and HFrEF-cAF patients. N-numbers indicate number of patients. P-values are based on one-way ANOVA with Tukey's multiple comparisons test.